Tampere University

Mikko Rautasalo

ANALYSIS OF MITIGATION METHODS FOR SHEATH VOLTAGES AND SHEATH CIRCULATING CURRENTS ON MEDIUM VOLTAGE WIND FARM COLLECTOR SYSTEM

Faculty of Information Technology and
Communication Sciences
Master of Science Thesis
December 2020

ABSTRACT

Mikko Rautasalo: Analysis of mitigation methods for sheath voltages and sheath circulating currents on medium voltage wind farm collector system
Master of Science thesis
Tampere University
Master's Degree Programme in Electrical Engineering
December 2020

Installed power on wind farms as well as their energy production are constantly increasing in order to achieve efficient utilization of the location where they are constructed. As a result, the power transferred in the wind farm collector systems is growing. This has resulted in excessively high sheath circulating currents and sheath voltages in the power cables. In addition to this, issues with problematical sheath connections are leading to insulation failures inside cable joints within wind farm medium voltage collector systems.

The objective of this thesis was to review and to develop methods to determine the magnitudes of sheath circulating currents and voltages. Furthermore, other goals were to determine the technical withstand limit of the collector system to these sheath circulating currents and to evaluate methods to decide if mitigation methods are required.

This thesis presents the current status for the problems dealing with the sheath connections and introduces the theoretical background of sheath circulating currents and sheath voltages. Methods to determine the magnitudes of these undesirable phenomena are presented, implemented, and evaluated.

Two case study wind farms based on actual design layouts were used to evaluate the results for the proposed calculation methods of sheath voltages and currents on power cables. Main focus was concentrated on the determination of the impact exerted on the power cable system through the implementation of mitigation methods or so-called cable screen bonding methods. This impact is numerically translated into resulting sheath voltages and currents, under different operational conditions, for instance with or without bonding systems.

Furthermore, the sheath circulating currents were calculated before and after implementing cross-bonding by using DIgSILENT PowerFactory simulation tool. With this tool, a more detailed model of the power cable can be done based on the cable structure and geometrical dimensions. In addition, this tool enables the consideration of the results from the power flow calculations done for different operational settings such as reactive power settings. One key finding using this grid simulation tool has been the influence of capacitive currents on the power cable to the resulting total sheath currents.

In addition, a sheath current measurement campaign was commissioned for the first case study wind farm before the integration of mitigation methods and obtained data were presented. A peak value of 60 A for the sheath current was observed, followed by a 40 A sheath current flow for a two-hour period. After this period, the cable experienced a joint failure leading to a total outage for the whole wind farm.

Moreover, external laboratory investigations were performed on these failed joints. The results indicated that the joints have experienced high sheath circulating currents. According to the findings, impurities have been left inside the joints resulting in oxidization within its metallic layers leading to insufficient contact between the cable sheaths and the joint braids.

Based on the measurements and laboratory results presented in this thesis, a recommended maximum sheath circulating current level of 40 A is proposed. By exceeding this proposed limit, the design for a wind farm collector system shall integrate cable sheath bonding methods as mitigation measures.

Keywords: Sheath voltage, sheath circulating current, medium voltage cable, solid bonding, single point bonding, cross bonding, DIgSILENT PowerFactory

TIIVISTELMÄ

Mikko Rautasalo: Analyysi tuulivoimapuiston keskijännitekaapelijärjestelmän kosketussuojien jännitteiden ja kiertävien virtojen ehkäisemisestä
Diplomityö
Tampereen yliopisto
Sähkötekniikan tutkinto-ohjelma
Joulukuu 2020

Tuulivoimapuistojen asennettu teho ja niiden energiantuotanto kasvavat jatkuvasti, jotta niiden sijainti voidaan hyödyntää tehokkaasti. Tuulivoimapuistojen kehityksen tuloksena niiden keskijännitekaapelijärjestelmissä siirretty teho on kasvussa. Tämä on johtanut liian suuriin kosketussuojien kiertäviin virtoihin sekä jännitteisiin kaapeleissa. Yhdessä ongelmallisten kosketussuojien liitäntöjen kanssa, suuret kosketussuojien kiertävät virrat aiheuttavat eristysvikoja tuulivoimapuistojen keskijännitekaapelijärjestelmien jatkoksissa.

Tämän diplomityön tavoitteena on tarkastella ja kehittää menetelmiä kosketussuojien kiertävien virtojen ja jännitteiden määrittämiseksi. Lisäksi tavoitteina on määrittää keskijännitekaapelijärjestelmän tekninen kestoraja kosketussuojien kiertäville virroille ja arvioida menetelmiä, joiden perusteella päätetään, tarvitaanko järjestelmässä erityisiä menetelmiä näiden virtojen ja jännitteiden rajoittamiselle.

Tämä diplomityö esittelee kosketussuojien liitosten ongelmallisen nykytilan sekä kosketussuojien jännitteiden ja kiertävien virtojen teoreettiset taustat. Lisäksi diplomityössä esitellään, käytetään ja arvioidaan näiden ei-toivottujen ilmiöiden määrittämismenetelmiä.

Kahta tuulivoimapuistoa, jotka perustuvat todellisiin suunnitelmiin, käytettiin arvioimaan kaapelien kosketussuojien jännitteiden ja kiertävien virtojen ehdotettujen laskentamenetelmien tuloksia. Pääpainona oli kosketussuojien jännitteiden ja kiertävien virtojen rajoittamismenetelmien eli kosketussuojien maadoitusmenetelmien toteuttamisen vaikutukset kaapelien kosketussuojien kiertävien virtojen ja jännitteiden suuruuteen. Nämä vaikutukset määritettiin laskemalla.

Kosketussuojien kiertävät virrat laskettiin ennen kosketussuojien vuorottelun toteuttamista sekä toteuttamisen jälkeen käyttämällä DIgSILENT PowerFactory simulointityökalua. Tämän simulointityökalun avulla kaapelijärjestelmän tarkan mallin luominen on mahdollista, käyttämällä kaapelin todellista rakennetta ja geometrisia mittoja. Simulointityökalu mahdollistaa myös tehonjaon laskennan eri käyttöasetuksilla, esimerkiksi loistehoasettelulla. Simulointityökalulla saavutettiin yksi diplomityön tärkeimmistä havainnoista, joka oli kaapelin kapasitiivisten virtojen vaikutus kosketussuojien kiertävien virtojen suuruuteen.

Käytössä olevalle tuulivoimapuistolle toteutettiin kosketussuojien virtamittaukset ennen kosketussuojien vuorottelun asentamista ja näiden mittausten tulokset esiteltiin tässä diplomityössä. Mittausjakson aikana kosketussuojan virta saavutti 60 A huippuarvon. Mittausjakson lopulla kosketussuojan virta ylitti 40 A yhtäjaksoisesti kahden tunnin ajan, jolloin kaapelin yksi jatkoksista vioittui. Tämä vika johti koko tuulivoimapuiston tuotannon pysähtymiseen.

Rikkoutuneelle jatkokselle suoritettiin tutkimukset ulkopuolisessa laboratoriossa. Näiden tutkimusten tulokset osoittivat, että jatkoksessa on kulkenut korkeita kosketussuojien kiertäviä virtoja. Lisäksi jatkoksen sisältä löydettiin epäpuhtauksia, jotka olivat aiheuttaneet jatkoksen metallisten kerrosten hapettumista. Hapettumisesta takia, kaapelin kosketussuojien ja jatkoksen liitospunosten välinen johtavuus oli heikentynyt.

Mittausten ja laboratoriotutkimusten tuloksien perusteella kosketussuojien kiertävien virtojen tekniseksi kestorajaksi ehdotetaan 40 A. Tämän rajan ylittyessä on suositeltavaa asentaa kosketussuojien maadoituksen erikoismenetelmä tuulivoimapuiston keskijännitekaapelijärjestelmään, joka sisältää jatkoksia.

Avainsanat: Kosketussuojien jännite, kosketussuojien kiertävät virrat, keskijännitekaapeli, tuulivoimapuiston kaapelijärjestelmä, kosketussuojan maadoitus, kosketussuojien vuorottelu, DIgSILENT PowerFactory

PREFACE

This Master of Science thesis was written as an assignment given by ABO Wind and it was part of a practical implementation of the content. The practical implementation was done during the year 2019 and the thesis was written as a post-work by December 2020.

I would like to give special thanks to my supervisor César Quintero Marrone, examiners Ari Nikander and Pertti Pakonen, and to Maysam Tahmasbi Afshar for the guidance and advice during my thesis project. I would also like to thank Aapo Koivuniemi, Norman Fischer and Marcelo Ariel Rothschild for the opportunity of doing this thesis.

Tampere, 14th December 2020

Mikko Rautasalo

CONTENTS

LIST OF FIGURES

LIST OF SYMBOLS AND ABBREVIATIONS

EU	European Union
U.S.	The United States of America
IRENA	International Renewable Energy Agency
PPA	Power Purchasing Agreement
MV	Medium Voltage
IEEE	Institute of Electrical and Electronics Engineers
Std.	Standard
CIRED	International Conference on Electricity Distribution
ENA	Energy Networks Association
CIGRE	International Council on Large Electric Systems
Emf	Electromotive force
WTG	Wind Turbine Generator
XLPE	Crosslinked polyethylene
ONAN	Oil Natural Air Natural
ONAF	Oil Natural Air Forced
XLPE	Cross-linked polyethylene
Al	Aluminium
GCC	Ground Continuity Conductor
MV	Medium Voltage
WF	Wind Farm
SS	Substation

I_m	Sheath current
I_n	Nominal Conductor current
$\overline{U}_{sa}$	Induced sheath voltage in sheath A
$\overline{U}_{sb}$	Induced sheath voltage in sheath B
$\overline{U}_{sc}$	Induced sheath voltage in sheath C
E	Sheath voltage gradient
K	Constant
S	Axial spacing of the phase conductors
d	Mean diameter of sheath
n	Constant
D	Mean diameter of sheath
ω	Angular velocity
V_{emf}	Electromotive force in volts
N	Number of turns in the circuit
ψ	Flux through each turn in the circuit
μ_0	Vacuum permeability
d_m	Diameter over the metallic sheath
R'_m	Sheath resistance / km
X'_m	Sheath reactance / km
$cos\varphi$	Power factor
$U_{L\text{-}L}$	Phase to phase voltage level of the medium voltage collector system
I_a	Nominal current flowing in phase conductor A
I_b	Nominal current flowing in phase conductor B
I_c	Nominal current flowing in phase conductor C
$U_{sa,tot,solid}$	Total sheath induced sheath voltage in phase A
$U_{sb,tot,solid}$	Total sheath induced sheath voltage in phase B
$U_{sc,tot,solid}$	Total sheath induced sheath voltage in phase C
I_A	Simulated current flowing in conductor of phase A
I_B	Simulated current flowing in conductor of phase B
I_C	Simulated current flowing in conductor of phase C

I_{sa}	Simulated current flowing in sheath of phase A
I_{sb}	Simulated current flowing in sheath of phase B
I_{sc}	Simulated current flowing in sheath of phase C

1. INTRODUCTION

In this chapter, the problems and background for sheath voltages and circulating currents are presented, and the purpose and goals of this thesis are explained.

1.1 Background

Wind energy has been a rapidly growing energy production type during the past 11 years. In the year 2009, the global cumulative installed wind capacity was 159 052 MW and it reached 651 000 MW in the year 2019. [1,2] One of the main drivers behind the rapid growth of wind energy, has been climate change. In the year 2011, the European Commission made a strategy for smart, sustainable, and inclusive growth. Part of the strategy was for member states to have committed themselves to reduce greenhouse gas emissions by 20 %, increasing the share of renewables in the EU's energy mix to 20 %, and achieving the 20 % energy efficiency target by 2020. [3]

To reach these goals, the world governments have been subsiding the wind energy growth directly with feed-in tariffs. The Finnish government set a feed-in tariff for 2500 MW of new capacity in the year 2011. Until the end of 2015, the feed-in tariff was 105,3 € / MWh and from 2016 until the end of 2017 it was 83,5 € / MWh. [4] The tariff systems made wind farms highly profitable which resulted in the construction of many new wind farms. To be as cost-efficient as possible these wind farms were built in the best locations possible, in other words, to areas with high wind expectations and where the grid is close by.

The rapid construction of new wind farms has already occupied a huge portion of the optimal locations. Therefore, wind farms are often developed further away from the grid, which has resulted in longer distances between the wind farms and common points of coupling.

As the installed capacity has been growing, so has the technology behind it. According to the Wind technology market report 2017 made by the U.S. Department of Energy and Office of Energy Efficiency & Renewable energy, the average nameplate capacity of the newly installed wind turbines in the United States in 2009 was approximately 1,72 MW and by the year 2017, it had increased to approximately 2,30 MW. [5]

The growth of the average nameplate capacity of the newly installed wind turbines can be seen even more clearly from ABO Winds' past constructed projects. In 2009 ABO Wind projects average nameplate capacity of the newly installed wind turbines was 2,0

MW and in 2017 it was 3,1 MW. In 2018 the average value increased only to 3,2 MW but new wind farms are going to be constructed with turbines between 4-6 MWs. [6]

The technological advancements in wind turbine generators are not just limited to the increase in the installed capacities. The wind turbine rotor diameters have been growing rapidly as well. The average rotor diameter of onshore wind farms was 67.4 m in the year 2005. The average rotor diameter grew steadily to 95.9 m in the year 2014. [7] New wind farms are currently developed by ABO Wind with turbines, which have rotor diameters up to 163 m.

To access higher wind speeds, the wind turbine tower hub heights have been rapidly growing as well. In Germany, the hub heights have increased by 80 % from 1998 to 2014. During the same period, the hub heights in Denmark increased by 110% and 49 % in the United States. In the year 2016 common hub heights of onshore wind turbines were 90-110m. New onshore wind farms are currently developed by ABO Wind with wind turbines, which have hub heights up to 169m. Due to these developments in technology, the wind farm yearly yields have grown significantly. This has resulted in higher currents flowing in the wind farm collector systems. [7,8]

The evolution of wind turbine technology has made the Wind Farm business highly profitable even without subsidies. According to IRENA The Power to Change: Solar and Wind Cost Reduction Potential to 2025 analysis the price of the onshore wind turbines have reduced 30-40% depending on the size of the project comparing the prices from 2009 to the prices from 2016. [8]

Modern Wind Farms are often financed with so-called power purchasing agreements (PPA). In these agreements, companies with high electricity consumption agrees to buy the electricity generated by the wind farm for a certain time and price. According to Wind Technologies Market Report 2018 made by the U.S. Department of Energy, the U.S. national average PPA prices topped in the year 2009 with above $70/MWh and in the year 2018 the price of the PPA's in the report's sample had reduced to $20/MWh. [9]

Many countries with mature markets, have given up the fixed tariff system, and instead the market is driven by tender processes. In Finland, the last tender was held in 2018. According to the tender results, the lowest bid for the tender was 31.37 €/MWh. [10]

1.2 Problem definition

The growing distances between wind turbines and points of common coupling, together with higher load currents in the Wind Farm transfer cables, have started causing undesirable phenomena in the Wind Farm medium voltage (MV) transfer cables. These undesirable phenomena are high sheath (metallic layer under the cable outer jacket) voltages, high sheath circulating currents, and an increasing amount of large cross-sectional cable joints needed in the medium voltage power cables.

The load current in the phase conductor induces a voltage to the cables metallic sheath. [11] The high sheath voltages introduce possibilities for potentially hazardous electroshocks to personnel. Regulators of many different countries have set permissible sheath voltage limits and recommendations to secure the safety of personnel. According to IEEE Std. 575-2014, the permitted sheath voltage levels are typically not higher than about 200 V. Although some utilities have allowed shield standing voltages up to 600 V. Finland among a few other European countries, is an exception regarding permissible sheath voltages. [12] The Finnish regulators have not set any limitations for the sheath voltages.

Sheath circulating currents consist mainly of capacitive and induced parts. Eddy currents are part of the sheath circulating currents as well, but their proportion of the whole circulating current is so small that Eddy currents are not considered in this thesis. [13]

The capacitance of the transfer cable causes continuous current to flow in the sheath under load and no-load conditions if the cable is energized. In a medium voltage cable, the current flowing in the main conductor produces a changing magnetic field around it. The cable sheath is exposed to this magnetic field and according to Faraday's law of induction, the changing magnetic field induces a current to the sheath, if the circuit is closed, in other words, if the cable sheath is grounded at least in two locations. [11]

Figure 1 presents the basic principle of induced circulating sheath current. In the Figure 1, I_m denotes the sheath current, I_n denotes the nominal conductor current

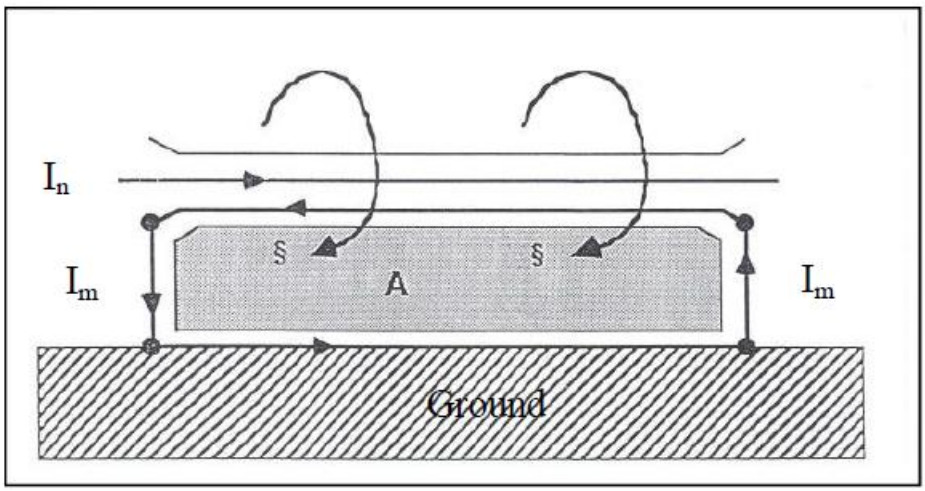

Figure 1. *Principle of induced screen current [14]*

These circulating currents cause losses in the cable sheath which results in a rise of the temperature of the cable. This temperature rise limits the ampacity of the cable. The heating can also damage the cable and eventually it can lead to failures. Specifically, the cable terminations and sheath connections in the joints might be damaged due to heated cable sheaths. These losses and possible failures lower the profitability of the wind farm. It must be noticed that the induced sheath currents may cause electroshocks for personnel as well. [14,15,16]

Similar problems have been experienced in medium voltage distribution networks in the past as well. In the year 2010, a research was published by Shanghai Municipal Electric Power Company and China State Grid Electric Power Research Institute. In this research circulating sheath current reached 26,6 A with a load current of 335 A in a 35 kV 630 mm^2 XLPE cable. In another study, sheath currents of 70 A has been measured on medium voltage XLPE cables with 50 mm^2 copper sheaths. [14,17]

Long distances between the Wind Farm and common point of coupling exposes the cable for greater sheath currents. The no-load condition sheath currents construct mostly of capacitive current. The magnitude of the capacitive current is directly proportional to the length of the cable. [11] The mitigation of circulating sheath currents is simulated and evaluated in this thesis.

The cable joints are possible and highly plausible fault locations if they are installed incorrectly or if the effects of the high sheath currents have not been considered and proper actions to mitigate them taken. [18] The growing cable lengths require multiple joints to be installed in the transfer cables. Due to the growing amount of power transferred in wind farm medium voltage cables, the cables cross-sections are growing. Hence, less cable can be fit in the cable drums, which results in a greater number of joints to be installed in the transfer cables.

The joints for large cross-sectional cables require precise installation methods and no errors are tolerated. Even small errors in the installation of the joint can result in poor connections between the cable and the joint. The poor connections together with high sheath currents cause heating and potentially electrical breakdowns of the insulation layers of the cables. Installation errors can also lead to uneven distribution of the electrical fields inside the joint, which will lead to unwanted partial discharge phenomenon. [19]

Partial Discharge reduces the lifespan of the cable due to the degradation of the insulation. If the electrical field strength is high enough, a breakdown of the insulation might occur. [20] The problems with transfer cable sheath connections exist due to a lack of standards for testing sheath connections, poor design, incoherent installation methods, incompetent personnel, and lack of information considering power cable installations. A CIRED Working group is currently analysing the problematic situation of the cable sheath connections. [18,21]

A practical example of problematic joints combined with high circulating sheath currents from a wind farm constructed by ABO Wind together with proper mitigation method is presented and evaluated in this thesis.

In many cases, a fault in the wind farm transfer cable automatically shuts down the whole wind farm. This happens due to on-shore wind farm collector systems being designed and constructed as radial-systems and often without N-1 reliability criteria. For example, all ABO Wind projects in Finland have been designed and constructed without the N-1 criteria so far. Depending on the case project, designing and constructing wind

farms with N-1 criteria could require huge capital investments, which could potentially make the project non-profitable.

In modern wind farms, the failures resulting from high sheath currents introduce huge economic losses if the effects of sheath circulating currents are not evaluated and possibly mitigated in the early phase of planning. When the project is designed according to the state of the art methods, the risk of economic losses due to failures will be minimized. Even average-size wind farms are big enough to cause 1000 € hourly yield losses. Economic compensations due to these described failures might be subject to liability and commercial litigation process between the affected parties.

Different methods to mitigate the described problems have been developed over the years. Special bonding methods to limit the sheath voltages and eliminate the induced circulating currents are presented and evaluated in this thesis. Practical examples exist in which implementing a special bonding method to a solid bonded system has reduced the sheath current from 50 A to 5 A. [14]

1.3 Objective and goals

The objective of this thesis is to review and to develop methods to determine the magnitudes of sheath circulating currents and voltages. Furthermore, other goals are to determine the technical withstand limit of the collector system to these sheath circulating currents and to evaluate methods to decide if mitigation measures are required.

The methods are to be used in the early phase of designing Wind Farms. When sheath currents are calculated with simulation tools in the early phase of designing, appropriate precautions can be defined, and they can be implemented to the cabling system design. [16]

In this thesis the sheath voltages of a wind farm are calculated before and after implementing mitigation methods. Sheath currents are simulated with the DIgSILENT PowerFactory simulation tool before and after implementing mitigation methods.

The calculations and simulations in this thesis focus on steady-state operational conditions. Transient overvoltages and faults are excluded from this thesis. The proximity effect is not in the scope of this thesis since it is not relevant in the steady-state operation. [16] In the dynamic simulation of sheath currents, the mutual influence of the different elements of the cabling system is considered.

1.4 Outline

Chapter 2 introduces the theoretical background to medium voltage cable sheath bonding methods. It depicts solid bonding, single-point bonding, and cross-bonding.

Chapter 3 introduces the theoretical background to medium voltage cable sheath voltages. It explains the phenomena, introduces limitations for the magnitudes, presents calculation methods for different bonding methods, and a basis for evaluating the need for mitigation.

Chapter 4 introduces the theoretical background to medium voltage cable sheath currents. It explains the phenomena, introduces practical reasons why the sheath currents occur in wind farm cabling systems, and present a calculation method to evaluate the sheath currents in solid bonded cabling systems.

Chapter 5 presents the simulation model of first case study wind farm built in DIgSILENT PowerFactory in order to calculate and analyse the sheath circulating currents and a special bonding method. The most important equipment and their implemented values are presented as well.

Chapter 6 presents faults that occurred in the first case study wind farm. It presents example of sheath voltage calculations for different bonding methods and analyses the results. It presents how sheath circulating current simulations were conducted. The simulation results are presented and analysed. Sheath circulating current measurement methods and results are presented and analysed.

Chapter 7 presents the most important finding of the thesis. It presents how to mitigate the problems described in chapter 1 and proposes a recommended limit for sheath circulating current.

2. MEDIUM VOLTAGE CABLE SHEATH BONDING METHODS

The purpose of the cable metallic sheath is to carry fault and charging currents during operation. In steady-state operation, the cable sheath also controls the electrical flux around the main conductor, forcing it to travel efficiently and evenly along the cable. [11,12]

The cable sheath bonding method has a significant impact on the induced voltages and on the circulating currents in the cable sheaths. Medium voltage transfer cable sheaths can be bonded in multiple different methods. Choosing the right bonding method depends mainly on the length of the cable, alignment of the cables, and on the current flowing in the conductors. [12]

The special sheath bonding designs must provide grounding for the cable and an uninterrupted return path for the fault currents via cable sheath and/or a ground continuity conductor. It must reduce steady-state sheath voltages and transient overvoltages to permissible levels, and significantly mitigate the sheath losses. [12]

The cable bonding system consists of the cable outer jacket, sheath interrupts, link boxes, and shield voltage limiters. Proper design and coordination between the components are necessary in order to have a functioning bonding system. [12]

When designing a special bonding system for Wind Farm transfer cables, the following aspects need to be considered. The cable sheaths should never be assumed to be at ground potential and proper precaution must be made to ensure the safety of the personnel. In practice, it is rare that the circulating sheath current is fully eliminated. It is then necessary to calculate the residual sheath currents and evaluate their effect on the cable ratings. [12]

2.1 Solid bonding

Solid bonding is a common type of bonding of the medium voltage cables. It has been widely used in distribution networks for safety reasons and the easy methods of installation. [14] In solid-bonding, the cable sheaths are connected together and then to the ground at both ends of the cable. [22] Figure 2 presents the solid bonding.

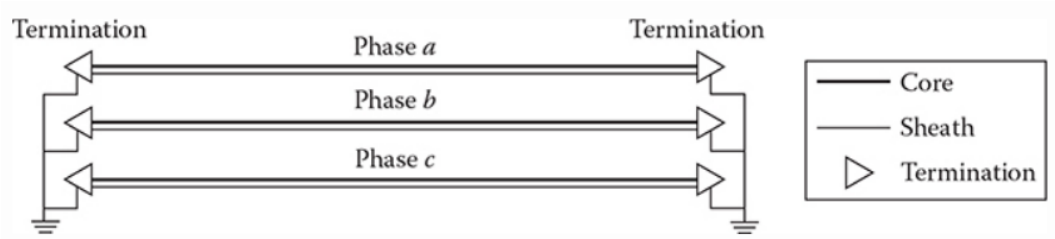

Figure 2. *Solid bonding of a cable [22]*

In single conductor cable circuits, solid bonding may expose the cable to high shield circulating losses when the conductors are carrying high loads. These losses can be excessive for the cable system and therefore problematic for the intended purpose. Medium voltage systems require analysing in the early phase of planning to determine if solid bonding is a viable option for the specific application. [12]

2.2 Single-point bonding

Single-point bonding is a special type of bonding in which one point of the cable is bonded to the ground. The three cable sheaths are connected together and then connected to the ground. In this type of bonding, a voltage is induced in the cable sheath. The induced voltage progressively increases as the distance from the grounding point increases. The maximum induced voltage is reached at the end of the cable, which is not grounded. In this type of installations, sheath voltage limiters should always be used at the cable end which is not grounded. [12]

Since the cable is not in direct contact with ground at both ends, a closed loop is not formed for the induced circulating currents to occur. This type of bonding is used in cables up to 2 km of length. In many countries, norms and standards apply specific limits for the shield voltages. These limits restrict the usage of single-point bonding in medium voltage cable systems. [12]

The Wind Farm transfer cable can be single-point bonded either at the end of the cable or in the middle of the cable route. Installing the single-point bonding to the middle of the cable route restricts the sheath voltages in the cable. Single-point bonding at the cable end is shown on top in Figure 3. Single-point bonding in the middle of the cable is shown on the bottom of the Figure 3. [12]

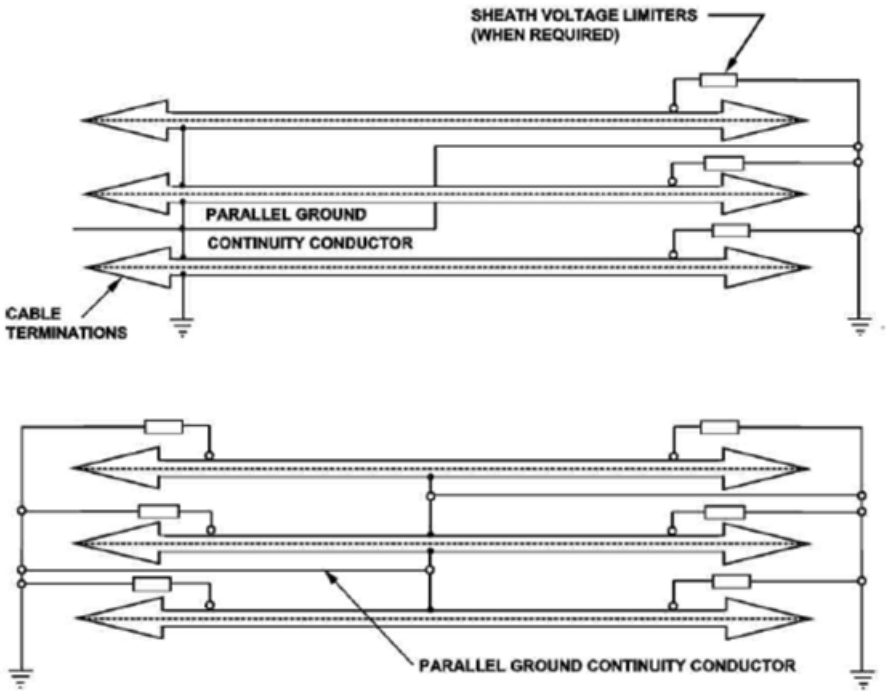

Figure 3. *Single-point bonding diagrams for circuits comprised of only one cable length [12]*

If a ground fault occurs in the Wind Farm cabling system, the zero-sequence current carried by the conductors returns by any path that is available. In single-point bonded medium voltage cable systems, the zero-sequence current cannot return by the cable sheath, since the cable is only grounded at one location. Therefore, the zero-sequence current flows through the ground if additional parallel grounding conductor is not available. [12]

The resistivity of the ground is very high in most cases, so the return current is widely diffused. Since the return path for the zero-sequence current is wide, high voltage is induced to parallel conductors. This could cause an appreciable potential difference between the ends of the transfer cabling system. For this reason, it is recommended to install a parallel grounding conductor to the cable trench, which is connected to the ground at both ends. This conductor's cross-section should be large enough to carry the expected fault current and it should be installed close enough to the cables to restrain the voltage in the cable sheath. [12]

If the cable system is long and cross-bonding is not possible, it might be considered to install multiple single-point bonding. For example, when the minor sections of the cable systems would be very unequal. This method requires an additional cable to be installed parallel to the phases. [12]

2.3 Cross-bonding

Cross-bonding is a special type of bonding in which the metallic sheaths of the three phases are cross-connected at least in two locations in such a way that the induced voltages and circulating currents are fully or partially eliminated. The cross-bonding locations are chosen in such a way that the cables are divided into equal-length minor sections. To fully eliminate the induced sheath voltages, the cables need to be transposed. Alternatively, the cables must be laid in trefoil formation, the conductors need to be transposed at each joint position, and the three minor sections must be equal length to fully eliminate the induced sheath voltages. Figure 4 presents the cross-bonding. [12]

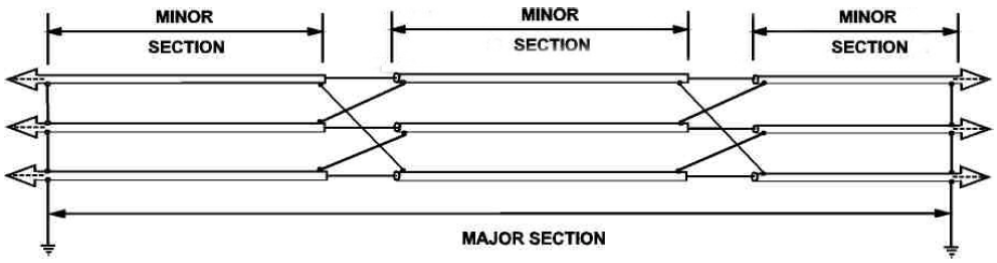

Figure 4 *Cross-bonded cables without transposition [12]*

Cross-bonding is generally the preferred bonding solution for Wind Farms which have long transfer cables or when the shield voltages become excessive due to very high fault currents. Cross-bonding should also be considered when the Wind farm installed capacity is high. Cross-bonding reduces losses and therefore it allows a smaller conductor size to be used in the transfer cabling system. [12]

When cross-bonding is installed to the Wind Farm transfer cabling system, a parallel grounding conductor is not necessary because the cable sheaths form a connection between the cable ends. Yet the parallel grounding conductor is often installed to ensure a low impedance, solid end to end connection. When the parallel grounding conductor is installed to the transfer cabling system, it must be considered that circulating currents might be induced to them which results in lower ampacity. To avoid these circulating currents, the parallel grounding conductor should be transposed if the cables are not transposed as shown in Figure 5. [12]

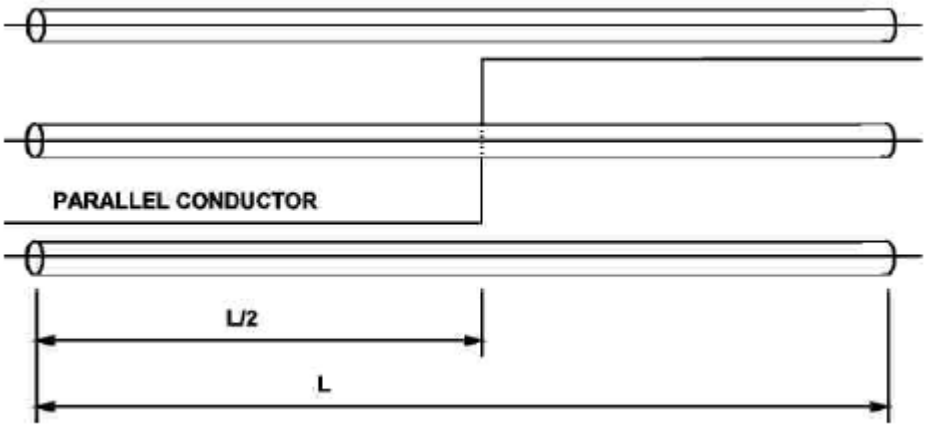

Figure 5. *Transposition of parallel ground continuity conductor to reduce induced shield/sheath voltages on power cables in flat or trefoil formation [12]*

Another advantage of cross-bonding compared to single-point bonding is the cable sheaths ability to operate better as a screening conductor during ground faults than a parallel grounding conductor. Therefore, the induced voltages in parallel objects such as cables, communication systems, pipes, fences are smaller during ground faults. [12]

The induced voltage in the cable sheath is approximately in phase with the current flowing in the conductor in a 3-phase cable system without cross-bonding. As described, the cable length is divided into three equal sections. In the first cross-bonding location the sheath of phase L1 is connected to the sheath of phase L2. Then on the second section, the load current of the L2 conductor induces the voltage in the sheath at 120° angle in respect to the previous one. At the second cross-bonding location the sheath of phase L2 will be connected to the sheath of phase L3. Then the load current of the L3 conductor induces the voltage in the sheath at 120° angle in respect to the previous section. [14]

The length of the section determines the magnitude of the induced voltage. Therefore, the section lengths must be equal to have the same voltage level in all phases and ideally resulting in zero voltage. Figure 6 presents the induced voltages in a symmetrical arrangement. [14]

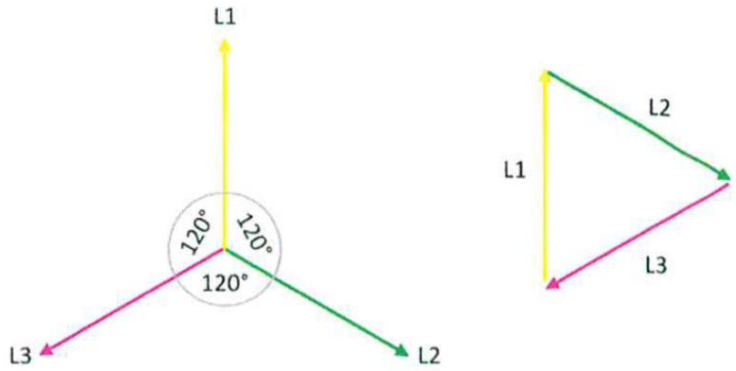

Figure 6. *Induced voltages in a symmetrical arrangement [14]*

In practice, it is almost impossible to achieve a fully symmetrical arrangement due to tolerances in installing and laying the cables. Therefore, a small voltage will be induced, and the current will flow in the cable sheath. However, the induced circulating current is significantly lower comparing to solid-bonded systems. According to Cross-bonding for MV cable systems study, practical experience has shown that in a solid-bonded system where a current of 50 A was measured on the cable sheath, the sheath current was reduced to 5 A after the implementing cross-bonding to the cable system. Figure 7 presents the Induced voltages in a non-symmetrical arrangement with a resulting voltage phasor. [14]

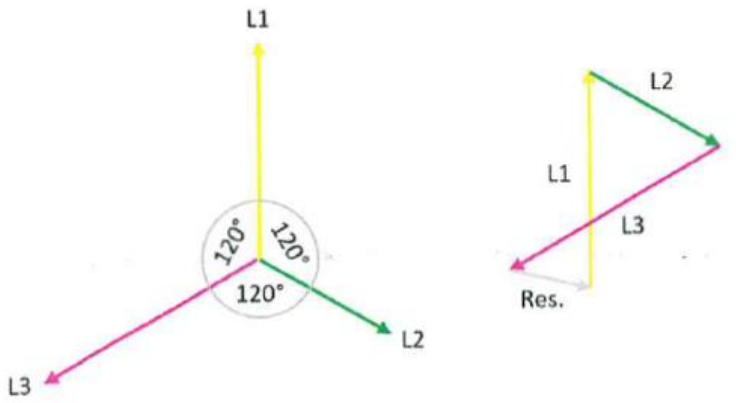

Figure 7. *Induced voltages in a non-symmetrical arrangement with resulting voltage arrow [14]*

To further limit the induced voltages of the minor sections, continuous cross-bonding can be implemented in the cable systems. The principle of continuous cross-bonding is the same as in regular cross-bonding, but the whole cable length is divided into a minimum of 4 minor sections instead of 3 minor sections. Although the minimum number of minor sections is 4, it is preferable to divide the whole cable length into minor sections divisible of 3. [12]

3. MEDIUM VOLTAGE CABLE SHEATH VOLTAGES

Undesirable sheath voltages occur in medium voltage underground cables measured between the cable sheath and ground due to conductors and sheaths mutual connection and inductive coupling. The main conductor and sheath's mutual connection happens due to the capacitive coupling effect which is also known as electrostatic coupling. In capacitive coupling electric field from the conductor couple to adjacent conductive objects, in this case to the cable sheath. The inductive coupling is caused by current flowing the phase conductor which produces a changing magnetic flux which induces a voltage to the cable sheath. [23]

The regulators in many countries have set limitations to the sheath standing voltages, since maintenance personnel may be exposed to contact to the cable sheaths. The personnel might not be aware of the existing sheath voltage and could assume it to be at ground potential. [15] Therefore, high sheath voltages may present a threat to the personnel.

The maximum permissible sheath voltage varies significantly between countries. Regulators in Finland have not set limitation to the sheath voltages, but the Finnish SFS 6001 high voltage electrical installations standard requires to deny contact to any part of the system which exceeds the touch voltage limitations set in the SFS 6001. [24]

Various recommendation for sheath voltages has been presented in the past literature. According to IEEE Std. 575-1988 the permissible sheath voltage in medium voltage cable sheath was at that time 65-90 V in the United States, but the evidence to verify these values was lacking. [15]

According to IEEE Std. 575-2014 until the 1990's it was common practice to limit the sheath voltages to 100 V in Canada. In France, the permissible sheath voltage limit was set to 400 V in the year 1994. Currently, in Great Britain it is common practice to limit the sheath voltages to 65 V. [12]

In this thesis, the sheath voltages are calculated in a medium voltage transfer cables of one case study wind farm currently being developed by ABO Wind and in other case study wind farm constructed by ABO Wind. Due to varying limitations in different countries and considering the non-existing limitations in Finland, the implementation of mitigation methods due to high sheath voltages is not considered as a main topic in this thesis for wind farms developed in Finland. For other countries, the recommendation of 65 V sheath voltage limit from United Kingdom's standard ENA C55-4 has been chosen for a basis to recommend implementing special bonding methods to reduce the sheath voltages. [25]

In balanced solid bonded systems, the inductive sheath voltages in unit length in the sheaths of single-core cables can be calculated by the methods and formulae recommended by the CIGRE Working Group 21 – 07. Equations 1-3 presents calculation methods for the induced sheath voltages for phases A, B, and C. [25]

$$\overline{U}_{sa} = j \cdot \omega \cdot I \cdot 2 \cdot 10^{-7} \cdot \left(-\frac{1}{2} + j \cdot \frac{\sqrt{3}}{2}\right) \cdot \ln\left(\frac{2 \cdot S}{d}\right) V/m \quad (1)$$

$$\overline{U}_{sb} = j \cdot \omega \cdot I \cdot 2 \cdot 10^{-7} \cdot \ln\left(\frac{2 \cdot S}{d}\right) V/m \quad (2)$$

$$\overline{U}_{sc} = j \cdot \omega \cdot I \cdot 2 \cdot 10^{-7} \cdot \left(-\frac{1}{2} - j \cdot \frac{\sqrt{3}}{2}\right) \cdot \ln\left(\frac{2 \cdot S}{d}\right) V/m \quad (3)$$

, where $\overline{U}_{sa}$ denotes the induced sheath voltage in sheath A, $\overline{U}_{sb}$ denotes the induced sheath voltage in sheath B, $\overline{U}_{sc}$ denotes the induced sheath voltage in sheath C, *I* denotes the nominal current flowing in the phase conductors, *ω* denotes the angular velocity, *S* denotes the axial spacing of the phase conductors, and *D* denotes the mean diameter of the sheath.

Figure 8 presents the trefoil burying arrangement of the single-core cables. Phase A is on the top, phase B is on the bottom left side, and phase C on the bottom right side.

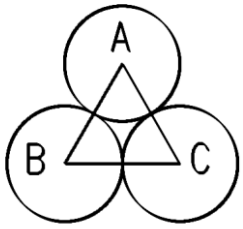

Figure 8. *Trefoil burying arrangement*

According to a paper written by ArresterWorks, the sheath voltage gradient in a single-point bonded system can be calculated with the equation 4. This equation has been derived from charts found in the IEEE Std. 575. [26]

$$E = k \cdot (\frac{S}{d})^n \quad (4)$$

, where *E* denotes the sheath voltage gradient in *V/km/kA*, *k* is a constant, *S* denotes the axial spacing of the phase conductors, *d* denotes the mean diameter of sheath, and *n* is a constant.

According to [26] for trefoil arrangement the equation 4 becomes as follows:

$$E = 75 \cdot (\frac{S}{d})^{0.466}$$

4. MEDIUM VOLTAGE CABLE SHEATH CURRENTS

In this chapter the sheath circulating currents occurring in medium voltage cable metallic sheaths are presented.

4.1 Capacitive sheath circulating current

The capacitive current occurring in the cable sheath is caused by capacitive coupling. As stated in the chapter 3, the main conductor and sheath's mutual connection happens due to the capacitive coupling effect which is also known as electrostatic coupling. This phenomenon raises the cable sheaths potential relative to ground potential by redistributing the electric charges within the cable sheath. [23]

The capacitive part of the sheath current is defined by the structure of the cable and by the length of the cable. The load current flowing in the main conductors does not contribute to the capacitive current. The capacitive current can be calculated by determining the capacitance per unit length and calculating the current per unit length with this determined value and sheath voltage. [11] In this thesis, the capacitive sheath current will be simulated and defined with no-load conditions before and after implementing cross-bonding in a wind farm constructed by ABO Wind.

In both ends bonded arrangement, the capacitive current flows from the phase conductor to the cable sheath and along the cable sheath to both directions. Depending on the cabling system parameters, such as sheath impedance and earthing impedance, the capacitive current can be unevenly distributed between the cable ends. [27]

Figure 9 presents the flowing path of the capacitive sheath current. In Figure 9, red arrows depict the capacitive current flowing path, point M depicts the first grounding location, K depicts a random point along the cable, N depicts the endpoint of the cable, and S depicts the second grounding location. [27]

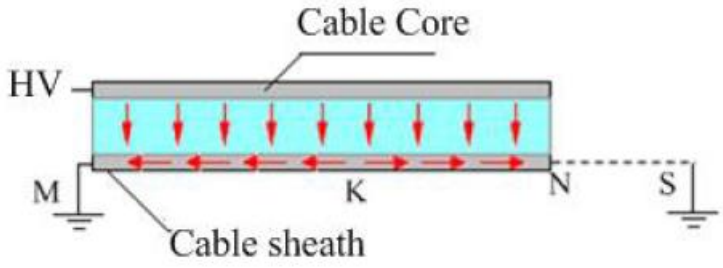

Figure 9. *Capacitance current under the crossbonded both-end grounding condition [27]*

4.2 Induced sheath circulating current

The induced sheath circulating current can be explained with Faradays Law of induction. According to Faradays Law of induction, a time-varying magnetic field generates an induced voltage, known as electromotive force (emf), which causes a current to flow in a closed circuit. Faraday's law can be written in equation form as in equation 5. [28]

$$V_{emf} = -\frac{d\lambda}{dt} = -N\frac{d\psi}{dt} \tag{5}$$

, where V_{emf} denotes the induced emf in volts, N denotes the number of turns in the circuit, ψ denotes the flux through each turn. The negative sign indicates that the induced voltage opposes the flux producing it, which is also known as Lenz's law. [28]

In wind farm medium voltage cable sheaths, a closed-circuit is formed when the cable sheath is connected to the earth in at least two different locations. Since a closed loop is required for the current to flow in the cable sheath, the induced sheath current is only relevant in solid- or cross-bonded cable systems, not in single-point bonded systems. Therefore, the circulating current in single-point bonded systems consists solely of the capacitive sheath current. [27]

In solid bonded cable systems, the total sheath current is the vector sum of the capacitive and induced currents. The angle between capacitive and induced parts is approximately the power angle. [27]

Excessive induced sheath circulating current can be caused by mixed burying arrangement methods of the cables or increased spacing between the conductors. In cables divided into multiple sections, as in cross-bonded systems, unequal lengths of the cable sections cause induced currents to flow in the sheath. [27]

In trefoil burying arrangement, the sheath circulating currents are equal in all phases. In flat formation burying arrangement, the magnitudes of the circulating currents are unequal. In flat formation the smallest magnitude occurs in the middle phase. This thesis focuses on the trefoil formation. [29]

The induced circulating sheath current can be calculated by dividing the induced sheath voltage with the total loop impedance. This loop impedance consists of the grounding impedance, the total sheath impedance, and impedance of possible connections along the cable including joints and terminations et cetera. [27] The magnitude of induced sheath circulating current depends on the induced voltage in the cable sheath, the total impedance of the circuit, the magnitude of the current flowing in the main conductor, and on the structure of the cable. [23]

A paper published in the 25th international Conference on electricity Distribution presents equation 6 to calculate the induced sheath circulating current in solid-bonded systems. [14]

$$I_m = \frac{I_n \cdot \omega \cdot \frac{\mu_0}{2\pi} \cdot \ln \frac{2a}{d_m}}{\sqrt{R'_m{}^2 + X'_m{}^2}} \tag{6}$$

, where I_m denotes the nominal current flowing in the conductor, a denotes the distance between cables, d_m denotes the diameter over the metallic sheath, R'_m denotes the resistance of cable sheath per unit length in km, X'_m denotes the reactance of cable sheath per unit length in km, ω is the angular velocity, μ_0 is the vacuum permeability.

5. WIND FARM SIMULATION MODEL

In this chapter, the first case study wind farm constructed by ABO Wind is presented. The wind farm consists of a substation, transfer cable, cable collector system, and wind turbine generators. There are 9 wind turbine generators whose maximum active power production is 3 MW per turbine. The voltage level at the medium voltage side of the wind farm is 33 kV. The frequency of the system is 50 Hz. The wind farm is connected to the 110 kV national grid.

Figure 10 depicts the solid bonded simulation model built in the DIgSILENT Power-Factory simulation tool. The wind turbine generator (WTG) medium voltage busbars are collected and connected to the master wind turbine generator 3 busbar. From the WTG 3 busbar, the whole power output of the wind farm is transferred to the medium voltage busbar of the substation using 800 mm^2 XLPE medium voltage cable. The length of this transfer cable is 11 420 m and it is buried 80 cm below the ground surface.

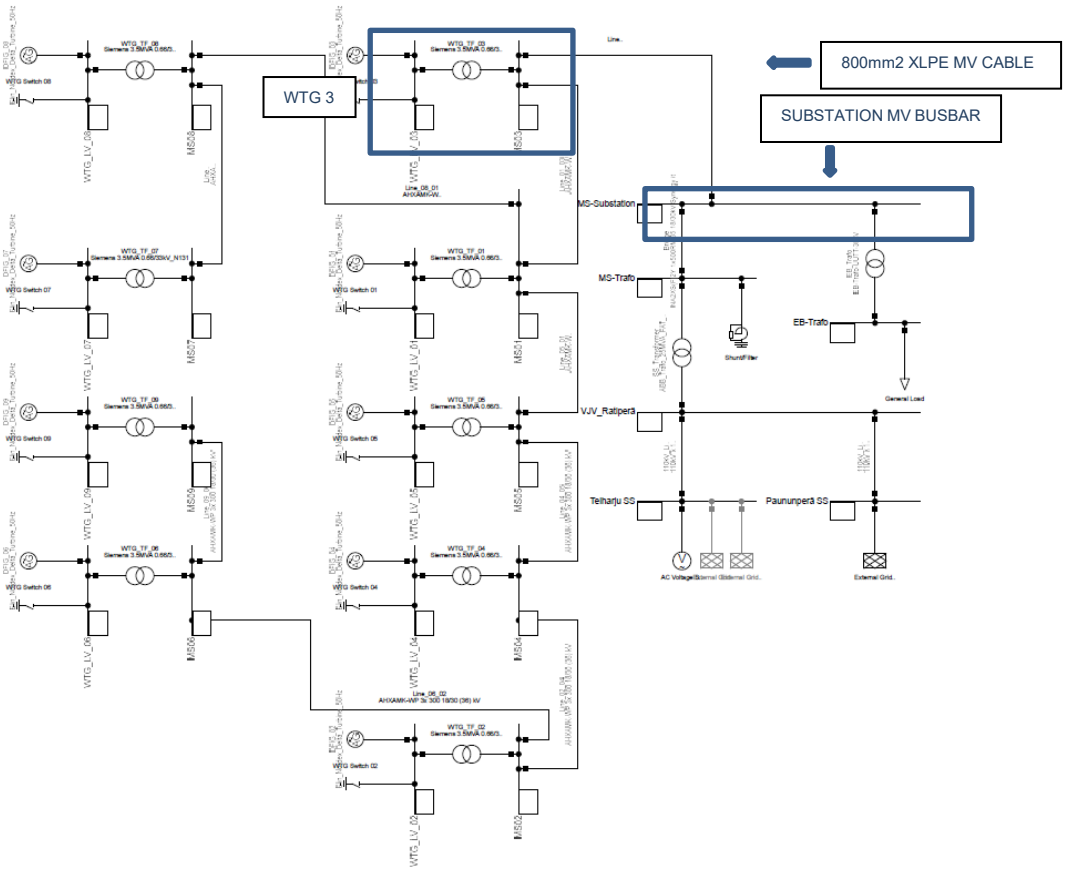

Figure 10. *Solid-bonded simulation model in DIgSILENT PowerFactory*

5.1 Wind turbine generators

The wind turbine generators in the first case study wind farm have doubly-fed induction generators that are connected to the collector system via 3500 kVA, Dyn5 step-up transformers. The voltage levels are 0.66 kV on the generator side and 33 kV on the collector system side. The short-circuit voltage for the transformers is 6% and copper losses 17 kW. The no-load current is 0.32 % and no-load losses 6.7 kW. The transformers have tap-changers with 2.5 % additional voltage per tap. The wind turbine generator step-up transformer values are presented in Table 1. These values have been applied to the simulation model in PowerFactory.

Table 1. *WTG Step-up transformer values*

Apparent power (kVA)	Vector group	Transformer ratio (kV)	Short circuit voltage (%)	Copper losses (kW)	No-load current (%)	No-load losses (kW)
3500	Dyn5	0.66/33	6	17	0.32	6.7

5.2 Power transformer

The first case study wind farm is connected to the national grid via one power transformer. The rated power of this power transformer at the wind farm substation is 25/31.5 MVA depending on the cooling method ONAN/ONAF. In this wind farm, the power transformer is used with the forced ventilation mode ONAF. The rated voltage at the transformer high voltage side is 118 kV and on the low voltage side 33.0 kV. The vector group is YNd11. The short-circuit voltage is 9.94 % and the copper losses are 77.645 kW. The no-load current is approximately 0.0938 % and the no-load losses are 12.879 kW. The values of the wind farm power transformer are presented in Table 2. These values have been applied to the simulation model in PowerFactory.

Table 2. *Wind farm power transformer values*

Apparent power ONAF (MVA)	Vector group	Transformer ratio (kV)	Short circuit voltage (%)	Copper losses (kW)	No-load current (%)	No-load losses (kW)
31.5	YNd11	33/118	9.94	77.645	0.0938	12.879

5.3 Wind farm collector system

The purpose of the Wind Farm transfer cabling system is to carry the power produced by the turbines from the Wind Farm to the grid. The first case study wind farm transfer cables are designed as 3 phase systems. The chosen voltage level of the system depends on the amount of power that is being transferred in the system. Modern Wind

Farm installed capacities tend to be so high that it is more efficient to choose a 33 kV voltage level instead of 20 kV due to the higher current carrying capacity in 33 kV systems. In the first case study wind farm the collector system's voltage level is 33 kV.

The transfer cabling system consists of medium voltage cables, straight through joints, sheath sectionalizing joints, protection devices, sheath voltage limiters, bonding leads, ground continuity conductors, terminations, cross-bonding link boxes, and earthing rods.

The effects of high circulating sheath currents must be considered when designing wind farm collector systems. By defining these effects, proper actions to mitigate them can be implemented in the early phase of planning if necessary. [16]

5.3.1 Medium voltage power cables

Cable manufacturers offer various types of XLPE power cables to be used in modern Wind Farms. AHXAMK-W and AHXAMK-WP medium voltage power cables are commonly used in Finland. These cables are longitudinally and radially waterproof. The structure of single-conductor AHXAMK-W cable is presented in Figure 11. Cable manufacturer Reka's single conductor AHXAMK-W 18/30 (36) kV cable is presented in Appendix 1. [30]

Figure 11. *AHXAMK-W cable structure [30]*

1. Conductor
2. Conductor screen
3. Insulation
4. Insulation screen
5. Swell tape
6. Aluminium laminate sheath
7. Outer jacket

In the first case study wind farm 3 different sizes of medium voltage XLPE cables are used. The connections between the wind turbine generators are implemented with single-core 630 mm^2 AHXAMK-W 18/30 (36) kV and 300 mm^2 AHXAMK-WP 18/30 (36) kV cables. The connection between the wind farm master turbine and the substation is implemented with single-core 800 mm^2 AHXAMK-W 18/30 (36) kV cable. Ground continuity conductors with a cross-section of 25 mm^2 are installed next to phase C. These conductors provide a solid path for the fault currents.

The structural measures of the 800 mm^2 AHXAMK-W cable are presented in Table 3. These values have been applied into the simulation model. The nominal diameter of the phase conductor is 33.3 mm. The nominal thickness of the semiconducting cross-linked polyethylene conductor screen is 0.5 mm. The nominal thickness of the cross-linked polyethylene insulation layer is 8.0 mm. The nominal thickness of the semiconducting cross-linked polyethylene insulation screen is 0.5 mm. The nominal thickness of the aluminium foil sheath is 0.3 mm. The nominal thickness of the oversheath is 2.8 mm.

Table 3. *800mm^2 AHXAMK-W structural dimensions*

Cross-section (mm^2)	**Conductor diameter (mm)**	**Conductor screen thickness (mm)**	**Insulation thickness (mm)**	**Insulation screen thickness (m)**	**Aluminium sheath thickness (mm)**	**Oversheath thickness (mm)**
800	33.3	0.5	8.0	0.5	0.3	2.8

5.3.2 Burying formations

Typically, medium voltage underground transfer cables are installed in the cable trenches in two different formations: trefoil- and flat formations. [31] The burying arrangement and spacing between the cables have a significant effect on the sheath circulating currents and heating of the cables. Increasing the spacing between the cables decreases the effects of mutual heating. However, increased spacing also increases the effect of electromagnetic coupling which results in higher circulating current losses and in lower ampacity. [15] Due to this fact, wind farm transfer cables are usually installed in tight trefoil arrangement.

In flat formation burying arrangement of three single-core cables, the three phases are installed in the same horizontal plane. In this arrangement, the outer phases are equidistant from the middle phase. Figure 12 presents the flat formation of the cables. [32]

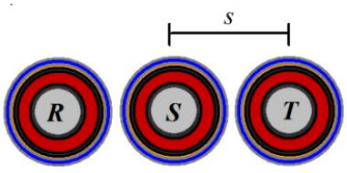

Figure 12. *Single-core cable layouts, flat formation [32]*

In the trefoil burying arrangement of three single-core cables, the three phases are installed in a way that the centres of the cables form an equilateral triangle. Figure 13 presents the trefoil formation. [32]

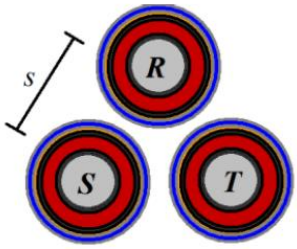

Figure 13. *Single-core cable layouts, trefoil formation [32]*

The trefoil burying arrangement is subjected to collapsing if not installed properly. To mitigate the collapsing of the arrangement, cable ties should be installed along the cable sections. In the first case study wind farm the cables are buried in trefoil formation.

5.3.3 Medium voltage cable joints

Two types of medium voltage cable joints are used in the first case study wind farm transfer cabling system. These are straight through and Sheath sectionalizing -joints. Straight through joints function in the transfer cabling system is to connect sections of transfer cable efficiently and reliably. Sheath sectionalizing joints' share the same purpose, but they also break the continuity of the cable sheaths and provide the possibility to cross-connect the sheaths. [12]

Cable equipment manufacturers offer multiple choices for medium voltage cable joints. The main difference between the joints is their shrinking method. The different shrinking methods are cold shrink, heat shrink, and hybrid. Also, the basic structure of the joint varies depending on the manufacturer and the shrinking method.

Cold shrink joints do not require additional heating to shrink the layers of the joint as the heat shrink joints do. Hybrid joints share the elements of both, heat- and cold shrink joints. Hybrid joints' inner layers are often cold shrinkable, and the outer layers are heat shrinkable.

Heat shrink joints require special skill and knowledge of the shrinking procedure to install them properly. In most cases, this is a disadvantage comparing to cold shrink joints, which layers are simpler to install. Cold shrink joints require higher ambient temperature when installed, which can be a disadvantage for example in Finland during the winter. In the first case study wind farm, the straight-through joints are hybrid joints and sheath-sectionalizing joints are heat shrink joints.

In the first case study wind farm, before implementing cross-bonding to the cabling system, the 800 mm^2 transfer cable consists of multiple sections, which are connected to each other with 14 hybrid straight joints. These hybrid joints include 25 mm^2 tinned copper braid. These braids connect the aluminium sheaths of the cable sections to each.

According to Finnish standard SFS 6000-2-52, Table B 52.2, 35 mm^2 copper is able to carry 130 A current when installed according to installation method D. [33] The maximum operating temperature according to the manufacturer is 90 degrees Celsius. The copper braid is connected to the cable aluminium sheath with a constant force spring.

5.3.4 Sheath voltage limiters and bonding leads

The purpose of sheath voltage limiters is to protect the cable sheath sectionalizing insulators and cable jackets from flashovers and punctures. These flashovers and punctures can be typically caused by lightning or fault transient overvoltages or switching surges. [12]

A commonly used sheath voltage limiter type in wind farm cabling systems is nonlinear resistance metal oxide varistor. The metal oxide varistor designs have a fast response to occurring transients, compact design and good AC voltage withstand recovery after a transient. Metal oxide varistors' conduction curve is divided into steep positive and negative linear resistance segments. [12]

Between the segments, the conduction current is very small as the voltage rises and as the applied voltage rises above a certain limit, the current increases rapidly due to small increases in the voltage. This effect, known as voltage clamping, shunts the overvoltages through the varistor. However, metal oxide varistors have a limited capacity to absorb energy and they are not designed to withstand internal 50 or 60 Hz fault currents. [12]

In single-point bonded cable systems, sheath voltage limiters are connected between the cable sheaths and ground at the cable end which is not directly grounded. Principally, the cable end, which is more likely to experience higher transient voltages, should be directly grounded. If the difference of ground resistance between the cable ends is very high, it is recommended that the lower resistance end is directly grounded. [12]

In cross-bonded systems in which the cables are directly buried, the cross-connecting of the cable sheaths are implemented inside link boxes. The sheath voltage limiters are located inside these link boxes which allows easy maintenance. The effectiveness of the sheath voltage limiters depends on the distance between the limiters and the cables since longer lead cables between the sheath voltage limiters and cable sheath introduce an additional voltage drop. [12]

The bonding leads should be low surge-impedance coaxial cable type and their length should not exceed 15 meters. Too long bonding leads may cause insulation failure in the sheath sectionalizing joint or cable jacket puncture. It must be considered that the bonding leads must withstand the system short-circuit currents. [12]

In the first case study wind farm, the cabling systems sheath voltage limiters are located inside the cross-bonding link boxes. The length of the bonding leads connecting the link boxes and sheath-sectionalizing joints are 5 m.

5.4 External grid

The first case study wind farm is connected to an external grid with a tap-in connection via the 33/110 kV power transformer. The voltage level in the external grid is 118 kV. The relevant values of the external national grid are presented in Table 4. The minimum short-circuit power is 99.59 MVA and the maximum 298.78 MVA. The minimum short-circuit current is 0.5 kA and the maximum 1.5 kA. The minimum short-circuit X/R -ratio is 2.5 and the maximum is 4.5. These values have been applied to the simulation model.

Table 4. *External grid values*

Voltage level (kV)		**Min. Short-circuit power (MVA)**	**Max. Short-circuit power (MVA)**	**Min. short-circuit current (kA)**	**Max. short-circuit current (kA)**	**Min. short-circuit X/R-ratio**	**Max. short-circuit X/R-ratio**
118		99.59	298.78	0.5	1.5	2.5	4.5

6. ANALYSIS

This chapter introduces joint failures experienced in the first case study wind farm. It presents an example of sheath voltage calculations for different bonding methods and analyses the results. It demonstrates how sheath circulating current simulations were conducted and the results are presented and analysed. Actual sheath circulating current measurement methods and results are presented and analysed.

6.1 Medium voltage joint failures

Medium voltage joint failures have happened in the first case example wind farm. These faults have been thoroughly investigated in different external laboratories. According to the results, the joints experienced insulation damage under the constant force spring of the hybrid joint.

The laboratory findings showed that the XLPE insulation of the cable was subjected to excessive heating close to the cables aluminium sheath. This indicates that high circulating currents have been flowing in the aluminium sheath.

In addition, oxidation of the outer surface of the cable aluminium sheath was found. Due to this oxidation, the conductivity of the aluminium sheath was significantly reduced. Therefore, the connection between the aluminium sheath and the joint copper braid was insufficient, which resulted in the heating of the connection under the constant force spring. Figure 14 presents the resulting puncture fault under the constant force spring.

Figure 14. *MV cable joint puncture fault under constant force spring*

State of the art installation methods demand that the cable ends prepared for jointing shall be kept clean and dry during the whole installation process. Any impurities left on the layers of the jointed cable could potentially lead to oxidation of the cable metallic sheath or the joint braid as the laboratory investigation has shown. In practice, the cables are often jointed in challenging terrain and weather conditions. Therefore, it is highly plausible that impurities invisible to human eye, are left inside the finished joint. The possibility that impurities will be left inside a joint increase as the number of joints increases.

From the laboratory results, it can be concluded that although the 25 mm^2 joint copper braids are designed to withstand the circulating sheath currents, the connection between the braid and the sheath does not always share the same capability. The connection is especially problematic if impurities has been left inside the joint close to the connection.

The problematic state of screen connections has been noticed by the CIRED as well. In a study presented in the 25th international conference on electricity distribution, it was stated that high circulating currents in the cable sheath can overload and damage the grounding connections of terminations and sheath connection in medium voltage joints. [14]

A study concerning the problems in the sheath connections has been presented in the 24th international conference & exhibition on electricity distribution as well. This study supports the problematic state of cable sheath connections presented in this thesis. The study stated that “Overheating of metallic ground screen connections at accessories of single cure cables are the root cause of severe insulation failures in the distribution network” [18]

6.2 Sheath voltages in a solid-bonded system

The first case study wind farm consists of 9 wind turbine generators whose maximum active power per turbine is 3.0 MW. The voltage level of the wind farm medium voltage collector system is 33 kV and the frequency is 50 Hz. The power factor of the collector system is 0.95. The length of the transfer cable between the master wind turbine generator and the wind farm substation is 11 420 km. The cable-type is single-core 800 mm^2 AHXAMK-W 18/30 (36) kV and it is buried in trefoil formation in such a symmetrical way that the phases are touching each other. Table 5 presents the relevant information of the MV collector system.

Table 5. *Collector system values*

Number of WTG's	WTG max. active power (MW)	Collector system voltage level (kV)	Collector system power factor	Frequency (Hz)
9	3.0	33.0	0.95	50

The nominal current flowing in the main conductors can be calculated with the equation 7.

$$I = \frac{P}{\sqrt{3} \cdot U_{L-L} \cdot \cos\varphi} \tag{7}$$

, where *I* denotes the nominal current flowing in the phase conductors, *P* denotes the maximum active power output of the wind turbine generator, $U_{L\text{-}L}$ denotes the phase to phase voltage level of the medium voltage collector system, and *cosφ* denotes the power factor of the collector system.

$$I = \frac{9 \cdot 3.0\ MW}{\sqrt{3} \cdot 33\ kV \cdot 0.95} = 497.239\ A$$

With a balanced load, the currents flowing in the conductors are I_a=I_b=I_c=I

As an example, the induced sheath voltages of the cable between the wind farm substation and master wind turbine generator are calculated using the equations 1-3. The axial spacing of the phase conductors is 59 mm and the mean diameter of sheath is 48.9 mm.

$$\overline{U}_{sa} = j \cdot 2 \cdot \pi \cdot 50\ Hz \cdot 497.239\ A \cdot 2 \cdot 10^{-7} \cdot \left(-\frac{1}{2} + j \cdot \frac{\sqrt{3}}{2}\right) \cdot \ln\left(\frac{2{\cdot}59\ mm}{48.9\ mmn}\right) = 0.027522 \angle -150\ V/m,$$

$$\overline{U}_{sb} = j \cdot 2 \cdot \pi \cdot 50\ Hz \cdot 497.239\ A \cdot 2 \cdot 10^{-7} \cdot \ln\left(\frac{2{\cdot}59\ mm}{48.9\ mm}\right) = 0.027522 \angle 90\ V/m,$$

$$\overline{U}_{sc} = j \cdot \omega \cdot 497.239\ A \cdot 2 \cdot 10^{-7} \cdot \left(-\frac{1}{2} - j \cdot \frac{\sqrt{3}}{2}\right) \cdot \ln\left(\frac{2{\cdot}59\ mm}{48.9\ mm}\right) = 0.027522 \angle -30\ V/m,$$

The magnitudes of total induced sheath voltages shall be calculated by multiplying the previously calculated values with the cable length 11 420 m. $U_{sa,tot} = U_{sa} \cdot l$

$$U_{sa,tot,solid} = 0.027522\,V/m \cdot 11\,420\,m = 314.301\,V,$$
$$U_{sb,tot,solid} = 0.027522\,V/m \cdot 11\,420\,m = 314.301\,V,$$
$$U_{sc,tot,solid} = 0.027522\,V/m \cdot 11\,420\,m = 314.301\,V,$$

, where $U_{sa,tot,solid}$ denotes the total sheath voltage in phase A in solid bonded arrangement, $U_{sb,tot,solid}$ denotes the total sheath voltage in phase B in solid bonded arrangement, and $U_{sc,tot,solid}$ denotes the total sheath voltage in phase C in solid bonded arrangement.

The results of sheath voltage calculations of the first case study wind farm are presented in Table 6.

Table 6. *Sheath voltage calculation results, solid-bonded first case study wind farm*

Induced sheath voltage per unit (V/m)	Cable length (m)	Sheath voltage of phase A (V)	Sheath voltage of phase B (V)	Sheath voltage of phase C (V)
0.027522	11 420	314.301	314.301	314.301

From the calculation results of the total induced sheath voltages, it can be deduced that the magnitudes are equal in all phases, since the load conditions are balanced, and the cables are buried in trefoil formation. It can be deduced that the sheath voltages greatly exceed the recommended 65 V. Therefore, it is recommended to implement cross-bonding to this cabling system.

6.3 Sheath voltages in a cross-bonded system

To maximize the advantage of implementing cross-bonding to the cabling system, the cable is divided into 3 equal length minor sections. The length for each section is therefore 3806.67 m. After implementing the cross-bonding, new sheath voltages are calculated using the same equations as in solid bonded systems. The new sheath voltages are the following:

$$U_{sa,tot,xb} = 0.027522\,V/m \cdot 3806.67\,m = 104.767\,V,$$
$$U_{sb,tot,xb} = 0.027522\,V/m \cdot 3806.67\,m = 104.767\,V,$$
$$U_{sc,tot,xb} = 0.027522\,V/m \cdot 3806.67\,m = 104.767\,V,$$

, where $U_{sa,tot,xb}$ denotes the total sheath voltage in phase A in cross-bonded arrangement, $U_{sb,tot,xb}$ denotes the total sheath voltage in phase B in cross-bonded arrangement, and $U_{sc,tot,xb}$ denotes the total sheath voltage in phase C in cross-bonded arrangement.

Implementing cross-bonding to the cable system, the sheath voltages reduce from 314.301 V to 104.767 V. From the calculation results it can be deduced that the induced sheath voltage does not fulfil the recommended 65 V before or after implementing cross-bonding to the cabling system. For countries with permissible sheath voltage limits, it is recommended to consider implementing continuous cross-bonding to further reduce the length of each minor section and therefore reduce the induced sheath voltages.

It must be considered that in practice it might not be possible to install cross-bonding to the optimal locations due to restriction of the terrain or permits. Unsymmetrical cable lengths would further increase the induced sheath voltages.

6.4 Sheath voltage in a single-point bonded system

The second case study wind farm, which is currently being developed by ABO Wind, is presented for the implementation of single-point bonding. This wind farm consists of 5 wind turbine generators whose maximum active power per turbine is 5.7 MW. The wind farm is divided into 2 systems. The first system includes 4 turbines and the second includes 1 turbine. The voltage level of the wind farm medium voltage side is 33 kV and the frequency is 50 Hz. The power factor of the system is 0.95 The length of the transfer cable between the first system and the wind farm substation is 894 m. The cable-type is single-core 800 mm^2 AHXAMK-W 18/30 (36) kV and it is designed to be buried in trefoil formation in such a symmetrical way that the phases are touching each other. The maximum current can be calculated with the equation 7 as follows

$$I = \frac{4 \cdot 5.7\ MW}{\sqrt{3} \cdot 33\ kV \cdot 0.95} = 419.891\ A$$

According to IEEE Std. 575-2014 single-point bonding should not be used in cable systems longer than 2 km. [12] Since the cable length is less than the recommended 2 km, single-point bonding can be considered for this project to mitigate the sheath circulating currents. Implementing single-point bonding to the cabling system reduces the induced sheath circulating current to zero but it increases the induced sheath voltage. [32]

When single-point bonding is implemented into a medium voltage collector system, the growing potential between the sheath and ground must be considered. As an example, the effect is calculated for the second case study wind farm.

Before implementing the special bonding method, the sheath voltage in the solid-bonded configuration is calculated with the equations 1-3. The increased sheath voltages are calculated as an example to evaluate if the recommended 65 V limit is exceeded.

$$\overline{U}_{sa} = j \cdot 2 \cdot \pi \cdot 50\,Hz \cdot 419.891\,A \cdot 2 \cdot 10^{-7} \cdot \left(-\frac{1}{2} + j \cdot \frac{\sqrt{3}}{2}\right) \cdot \ln\left(\frac{2{\cdot}59\,mm}{48.9\,mmn}\right) =$$
$$0.023241 \angle -150\,V/m,$$
$$\overline{U}_{sb} = j \cdot 2 \cdot \pi \cdot 50\,Hz \cdot 419.891\,A \cdot 2 \cdot 10^{-7} \cdot \ln\left(\frac{2{\cdot}59\,mm}{48.9\,mm}\right) = 0.023241 \angle 90\,V/m,$$
$$\overline{U}_{sc} = j \cdot \omega \cdot 419.891\,A \cdot 2 \cdot 10^{-7} \cdot \left(-\frac{1}{2} - j \cdot \frac{\sqrt{3}}{2}\right) \cdot \ln\left(\frac{2{\cdot}59\,mm}{48.9\,mm}\right) = 0.023241 \angle -30\,V/m,$$

The magnitudes of total induced sheath voltages shall be calculated by multiplying the values with the cable length 894 m. $U_{sa,tot,solid} = U_{sa} \cdot l$

$$U_{sa,tot,solid} = 0.023241\,V/m \cdot 894\,m = 20.778\,V,$$
$$U_{sb,tot,solid} = 0.023241\,V/m \cdot 894\,m = 20.778\,V,$$
$$U_{sc,tot,solid} = 0.023241\,V/m \cdot 894\,m = 20.778\,V,$$

The sheath voltage gradient in a single-point bonded system is calculated with the equation 4. To calculate the sheath voltage gradient, the axial spacing of phase conductors *S* and the mean diameter of the sheath are inserted to the equation.

$$E = 75 \cdot \left(\frac{59\,mm}{48.9\,mm}\right)^{0.466} V/km/kA = 81.858\,V/km/kA$$

To calculate the maximum sheath voltage, the sheath voltage gradient is multiplied by the cable length and the current flowing in the conductors on the maximum output of the wind turbines.

$$81.8579\,V/km/kA \cdot 0.894\,km \cdot 0.41981\,kA = 30.722\,V$$

From the calculation it can be deduced that implementing single-point bonding to the cabling system, the increased sheath voltage does not exceed the recommended limit of 65 V.

6.5 Circulating sheath currents

To determine the conductor currents and circulating sheath currents in the first case study wind farm, two wind farm models are built in the DIgSILENT PowerFactory simulation tool. DIgSILENT describes its PowerFactory software as a leading power system analysis software application for use in analysing generation, transmission, distribution, and industrial systems. The simulation software uses state-of-art solution algorithms. [34] The software is widely used at ABO Wind to calculate and analyse wind farm power flows and fault conditions.

In the first simulation model, the transfer cable between the wind farm master turbine generator and wind farm substation is solidly-bonded. In the second model, the transfer cable model is cross-bonded and the effects of implementing cross-bonding to the first case study wind farm are simulated.

To be able to simulate the induced currents in the wind farm transfer cable, the geometric arrangement of the cable and the link between cable system type and the line elements are created. PowerFactory calculates the impedance and admittance matrices of the arrangement and uses them to represent the system in the calculations. [35]

In addition, the equation 6 presented in the cross-bonding for MV Cable Systems: Advantages and Impact on Accessories paper by CIRED is qualitatively analysed.

6.5.1 Solid-bonded system simulations

The solid-bonded simulation model of the first case study wind farm is presented earlier in Figure 10. The model represents the actual implementation of the wind farm and its collector system before retrofitting cross-bonding to the external cable. The actual geometry of the cables and arrangements of phases is considered in the simulation model as depicted in chapter 5.

The simulation model of the solid bonded external cabling system is presented in Figure 15. The external medium voltage cable is coupled with the external cable aluminium sheath and the ground continuity conductor (GCC) running along the same trench between the wind farm master turbine and the wind farm substation.

The aluminium sheaths are connected to the ground at the substation end of the section via series resistance which depicts the actual earthing resistance at the substation. At the master turbine, the sheaths are connected to earth via series resistance which depicts the actual earthing resistance at the master wind turbine.

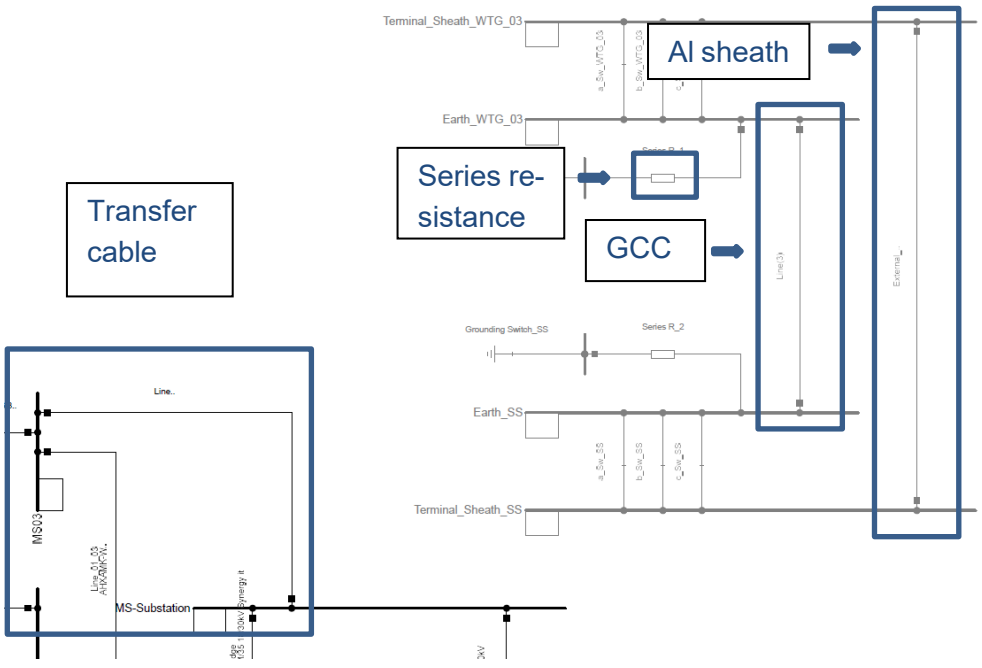

Figure 15. *Solid-bonded simulation model of external cable system in DIgSILENT PowerFactory*

Figure 16 presents the simulation results of conductor currents flowing in the cable between the master turbine and the substation at the wind farm end of the cable as vector phasors.

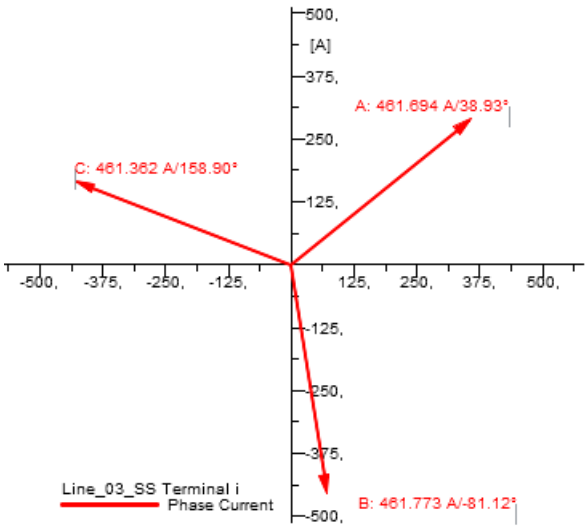

Figure 16. *Conductor current phasors in solid-bonded system, wind farm side*

According to Figure 16, the maximum magnitude of the conductor current at the wind farm side is approximately 461.8 A with maximum production.

Figure 17 presents the simulation results of conductor currents flowing in the cable between the master turbine and the substation at the substation end of the cable as vector phasors.

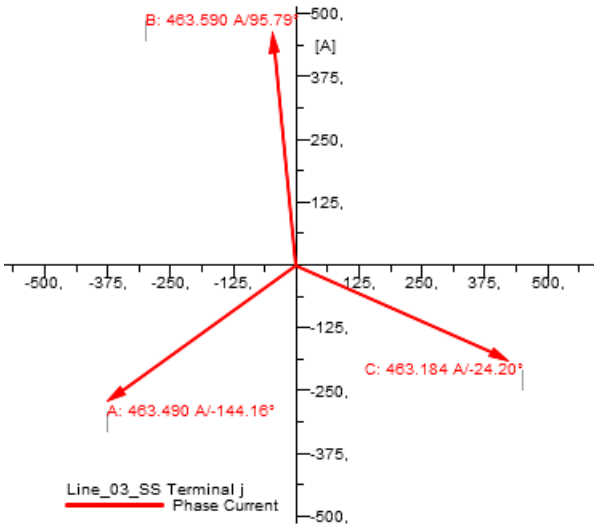

Figure 17. *Conductor current phasors in solid-bonded system with maximum production, substation side*

According to Figure 17, the maximum magnitude of the conductor current at the substation side is approximately 463.6 A with maximum production.

Figure 18 presents the simulation results of total sheath circulating currents flowing in the cable between the master turbine and the substation at the wind farm end of the cable as vector phasors.

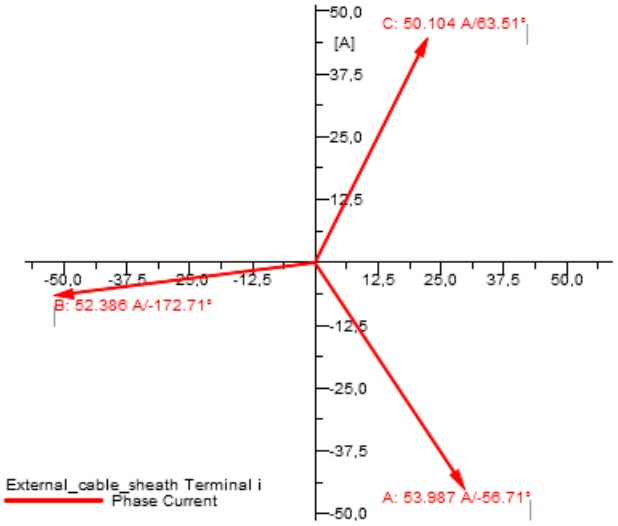

Figure 18. *Sheath current phasors in solid-bonded system with maximum production, wind farm side*

From Figure 18, it can be deduced that the magnitudes of the sheath circulating currents in each phase are not equal. The magnitude of the sheath circulating current in phase A is approximately 54.0 A, in phase B it is approximately 52.4 A and in phase C approximately 50.1 A.

The deviations in the magnitudes can be explained with the implementation of the cabling system. The ground continuity conductor is placed next to the phase C and it disturbs the symmetrical distribution of the induced currents. Hence, the induced circulating current in each phase increases as the distance from the ground continuity conductor increases. The simulation results are in line with the IEEE Std. 575-2014, which states that “The magnetic field resulting from current flow through the core conductor couples the metallic shield/sheath and any other adjacent conductors”. [12]

Figure 19 presents the same simulation results without a ground continuity conductor and proves that the magnitudes of sheath circulating current in each phase would be approximately equal without the ground continuity conductor.

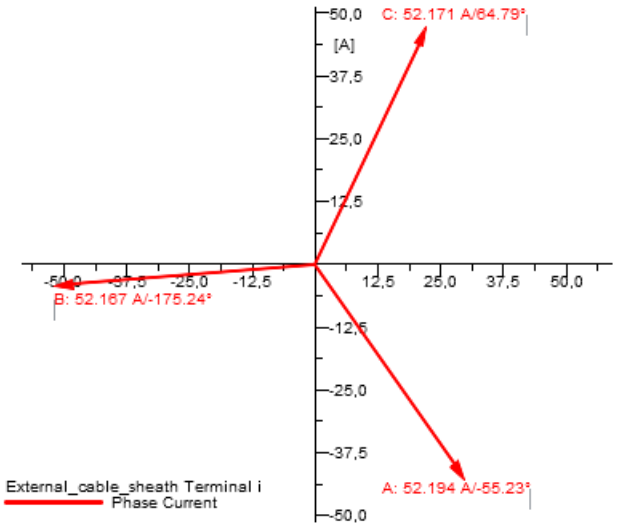

Figure 19. *Sheath current phasors in solid-bonded system with maximum production, wind farm side, without ground continuity conductor*

From Figure 19 it can be deduced that after removing the ground continuity conductor, the magnitudes of the sheath circulating currents are almost equal. The magnitudes of total sheath circulating currents are approximately 52.2 A in all phases.

Figure 20 presents the simulation results of total sheath circulating currents flowing in the cable between the master turbine and the substation at the substation end of the cable as vector phasors.

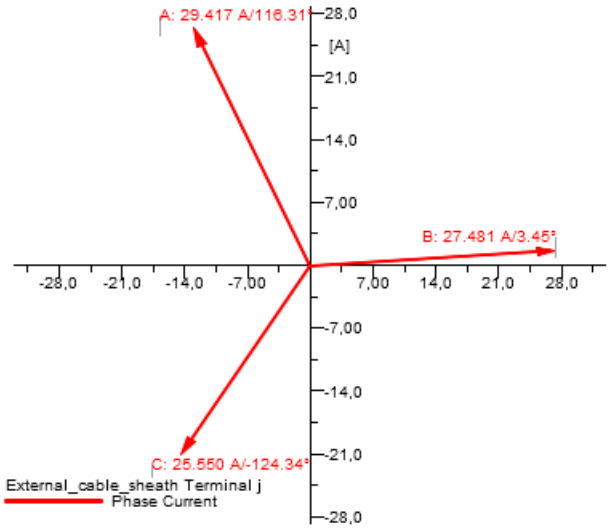

Figure 20. *Sheath current phasors in solid-bonded system with maximum production, substation side*

From Figure 20, it can be deduced that the magnitudes of the sheath circulating currents in each phase are not equal. The magnitude of the sheath circulating current in phase A is approximately 29.4 A, in phase B it is approximately 27.5 A and in phase C

approximately 25.6 A. The reason for the deviations between the sheath circulating current magnitudes in each phase at the substation side follow the same principle as at the wind farm side of the cable.

The conductor currents and the sheath currents are simulated for different output powers of the wind farm to evaluate the magnitude of sheath circulating currents with different conductor currents. Based on this evaluation, it is possible to conclude if special bonding methods are needed for the external cable system. The power generation of each turbine is adjusted from 0 MW to 3 MW with 0.5 MW steps.

In the 0 MW situation, the wind turbine generators are disconnected, hence no current is flowing in the conductors. In this situation, no current is induced to the cable sheaths. Hence, the leftover current occurring in the cable sheath depicts the capacitive part of the sheath circulating current.

The results of these simulations are presented in Table 7 and in *Figure* 21. Abbreviation WF refers to the wind farm and SS to the substation. The currents $I_{A,}$ I_B, and I_C denote the simulated currents flowing in conductors of corresponding phases. The currents I_{sa}, I_{sb}, and I_{sc} denote the simulated currents flowing in sheaths of corresponding phases.

Table 7. *Circulating sheath current simulation results, solid-bonded first case study wind farm*

WTGP injection (MW)	**Conductor current WF side (A)**			**Conductor current SS side (A)**			**Sheath current WF side (A)**			**Sheath current SS side (A)**		
	I_A	I_B	I_C	I_A	I_B	I_C	I_{sa}	I_{sb}	I_{sc}	I_{sa}	I_{sb}	I_{sc}
0	12.5	12.5	12.5	37.3	37.3	37.3	12.3	12.5	12.3	13.0	12.8	12.9
0.5	84.3	84.3	84.2	78.4	78.5	78.4	19.5	19.2	18.9	5.2	5.7	5.9
1.0	158.8	158.9	158.7	156.5	156.6	156.4	26.5	25.9	25.2	1.8	1.5	0.5
1.5	234.8	234.9	234.7	234.1	234.2	233.9	33.4	32.6	31.5	8.8	7.8	6.9
2.0	310.8	310.9	310.6	311.1	311.2	310.9	40.3	39.2	37.7	15.7	14.4	13.1
2.5	386.5	386.6	386.2	387.6	387.7	387.3	47.2	45.8	43.9	22.6	21.0	19.4
3.0	461.7	461.8	461.4	463.5	463.6	463.2	54.0	52.4	50.1	29.4	27.5	25.6

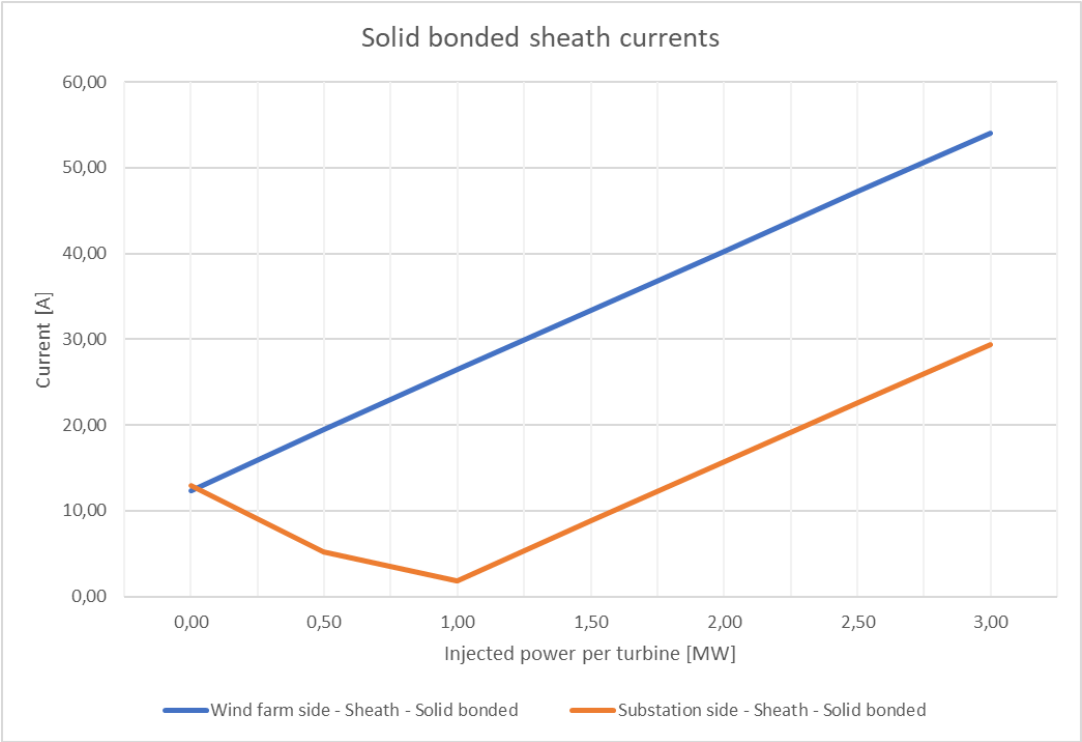

Figure 21 *Circulating sheath current simulation result figures, solid-bonded first case study wind farm*

From the simulation results, it can be concluded that the capacitive sheath circulating current is approximately 13 A according to the no-load condition. The simulation results indicate that the sheath circulating current is greater on the wind farm side of the cable.

When the turbines start to inject active power to the collector system, induced circulating current begins to flow in the cable sheaths. The total sheath circulating current is the vector sum of the capacitive and induced sheath circulating currents. [27] As the capacitive current flows from the middle of the cable towards both ends of the cable, the capacitive circulating current is out of phase with the induced current at the substation side of the cable and in phase at the wind farm side of the cable. Hence, the magnitude of total sheath circulating current on the substation side decreases until it reaches a critical point.

At the critical point, the induced current exceeds the capacitive current. After exceeding the critical point, the magnitude of the total sheath circulating current starts to increase. In the simulation, the critical point is reached after increasing the WTG active power injection from 1.0 MW to 1.5 MW.

On the wind farm side of the cable, the capacitive sheath circulating current flows in the opposite direction compared to the substation side of the cable. Hence, they are in phase with each other. Therefore, the magnitude of total sheath circulating current increases as the capacitive and induced sheath circulating currents are summed together. Though this reason does not fully cover the deviations between the magnitudes of the

total sheath circulating currents on the opposite sides of the cable. The earthing resistance at the substation is higher compared to the earthing resistance at the wind turbine. Hence, the sheath circulating current is higher on the wind farm side of the cable.

According to the simulation results, the magnitude of the current flowing in the conductors exceeds roughly 310 A as the magnitude of sheath circulating current exceeds the proposed sheath current limit of 40 A. Therefore, it is recommended to install cross-bonding to the first case study wind farm. The proposed sheath current limit of 40 A is discussed in chapter 6.6.

6.5.2 Solid-bonded system sheath current calculations

CIRED publication presents a simple equation to evaluate the induced sheath circulating currents in symmetrical solid-bonded systems. [14] When examining the equation 6, it can be deduced that the equation only considers the corresponding cable section and neglects all other parts of the cabling system.

$$I_m = \frac{I_n \cdot \omega \cdot \frac{\mu_0}{2\pi} \cdot \ln\frac{2a}{d_m}}{\sqrt{{R'_m}^2 + {X'_m}^2}}$$

Calculating the induced sheath circulating current should also consider other parts of the cabling system as well. The paper Sheath Circulating Current Calculations and Measurements of Underground Power Cables presented in the JICABLE 2007 states that the induced sheath circulating current can be calculated by dividing the sheath induced voltage by the total impedance in the loop circuit of the cable sheath. The total loop circuit impedance consists not only of the cable metallic sheath but also of the grounding impedance, and impedance of the connections of joints and terminations. [27] Therefore, caution should be taken while using equation 6 as a basis for evaluating the magnitude of induced sheath circulating currents in cabling systems.

It should also be noted that the equation 6 only considers induced part of the sheath circulating current. The total sheath circulating current consists of capacitive current as well. The simulation and measurement results presented in this thesis indicate that the capacitive current has a significant effect on the total sheath circulating current in long cable sections. Therefore, caution should be taken while using equation 6 as a basis for evaluating the need for implementing special bonding methods to the cabling system in order to mitigate the sheath circulating currents.

6.5.3 Cross-bonded system

Figure 22 presents the cross-bonded wind farm simulation model built in the DIg-SILENT PowerFactory. In the cross-bonded model, the transfer cable has been divided into 3 equal lengths minor sections. In the model, each section is separated with a terminal.

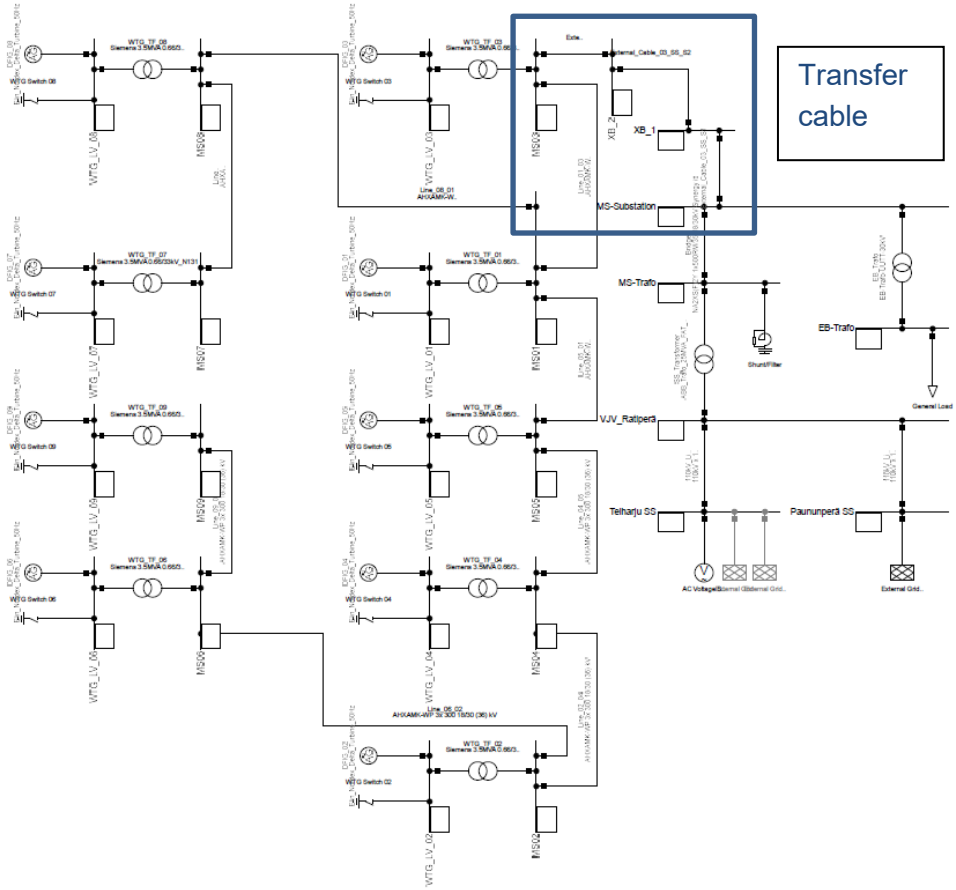

Figure 22. *Cross-bonded simulation model of first case study wind farm in DIg-SILENT PowerFactory*

Figure 23 presents the simulation model of the cross-bonded external cabling system. The external medium voltage cable is divided into 3 equal length minor sections. The cross-bonding boxes are simulated with 2 terminals at the end of each section along the line which represents the aluminium sheaths.

The transposition of the sheaths is implemented by cross-connecting the sheaths between the terminals. Each minor section of the cross-bonded transfer cable is coupled with the corresponding section of the aluminium sheath and the ground continuity conductor (GCC).

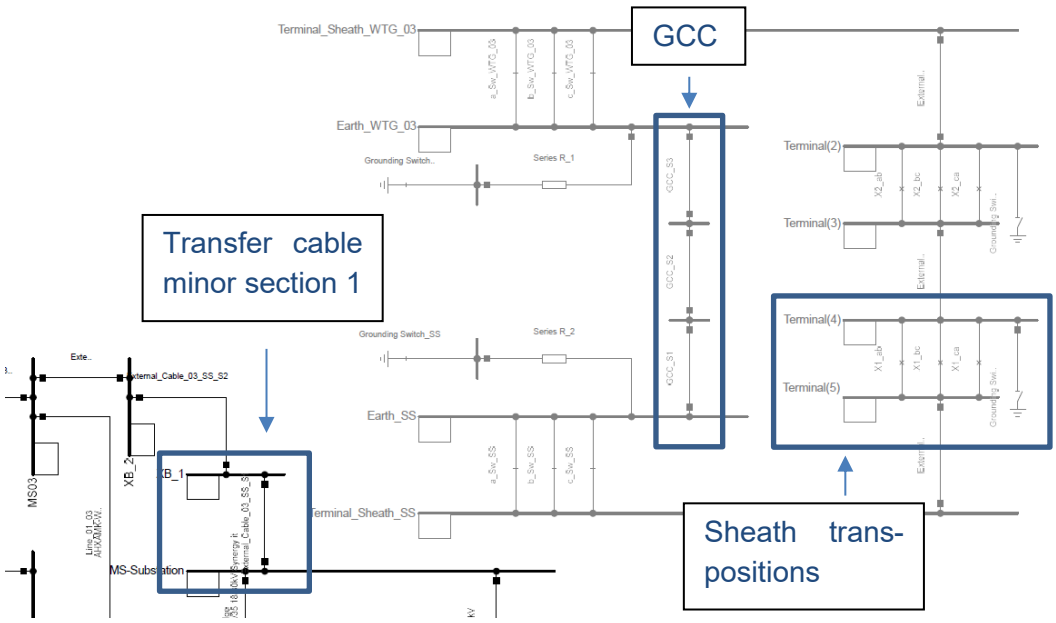

Figure 23. *Cross-bonded simulation model of external cable system in DIgSILENT PowerFactory*

Figure 24 presents the simulation results of conductor currents flowing in the cable between the master turbine and the substation at the wind farm end of the cable as vector phasors in cross-bonded arrangement.

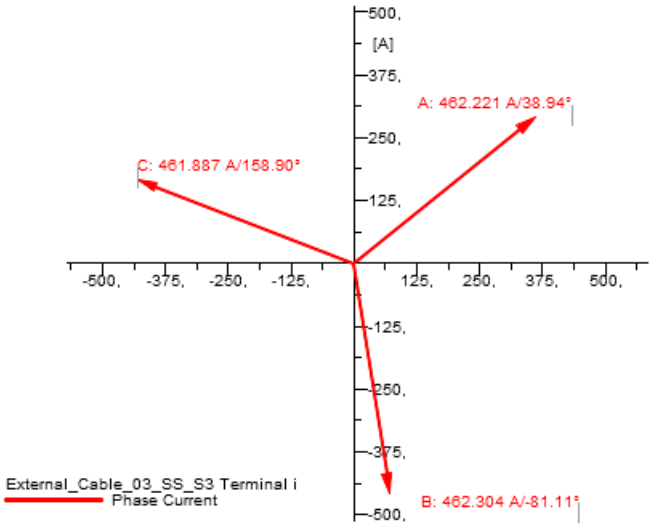

Figure 24. *Conductor current phasors in cross-bonded system with maximum production, wind farm side*

According to Figure 24, the maximum magnitude of the conductor current at the wind farm side is approximately 462.2 A with maximum production.

Figure 25 presents the simulation results of conductor currents flowing in the cable between the master turbine and the substation at the substation end of the cable as vector phasors in cross-bonded arrangement.

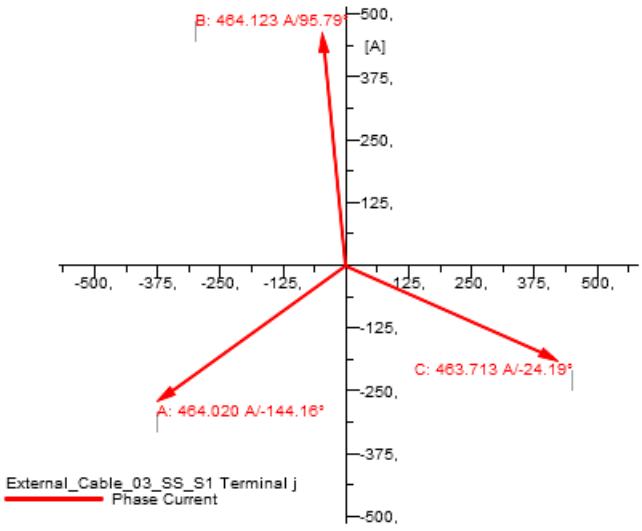

Figure 25. *Conductor current phasors in cross-bonded system with maximum production, substation side*

According to Figure 25, the maximum magnitude of the conductor current at the wind farm side is approximately 464.1 A with maximum production.

Figure 26 presents the simulation results of total sheath circulating currents flowing in the cable between the master turbine and the substation at the wind farm end of the cable as vector phasors in cross-bonded arrangement.

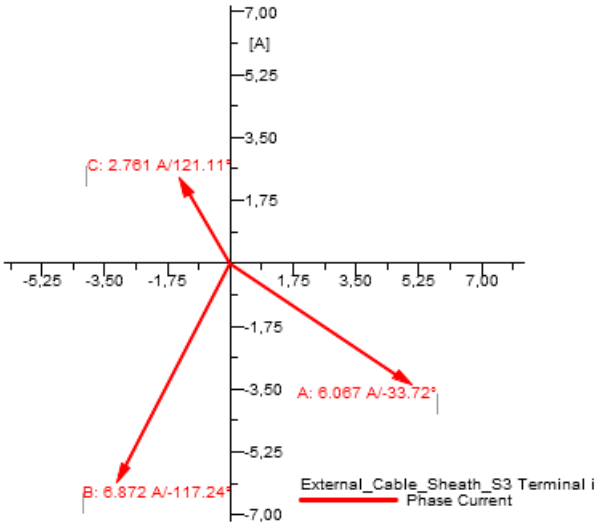

Figure 26. *Sheath current phasors in cross-bonded system with maximum production, wind farm side*

From Figure 26, it can be deduced that the magnitudes of the sheath circulating currents in each phase are not equal. The magnitude of the total sheath circulating current in phase A is approximately 6.1 A, in phase B approximately 6.9 A and in phase C approximately 2.8 A.

The deviations in the magnitudes can be explained with the implementation of the cabling system. The ground continuity conductor is placed next to the phase C on the wind farm side of the cable. As the sheaths of the cables are transposed in two locations, the ground continuity conductor is next to phase A sheath at the substation end of the cable. The ground continuity conductor disturbs the symmetrical distribution of the induced currents. Hence, the induced circulating current in each phase increases as the distance from the ground continuity conductor increases.

Figure 27 presents the same simulation results without a ground continuity conductor and proves that the magnitudes of sheath circulating current is each phase would be approximately equal without the ground continuity conductor

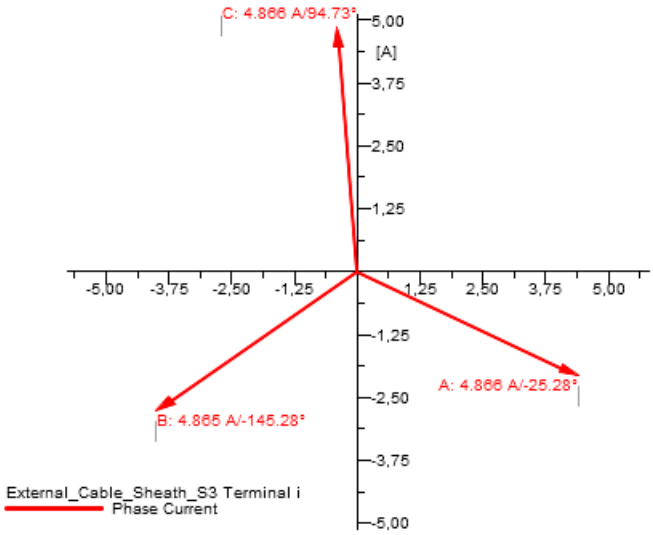

Figure 27. *Sheath current phasors in cross-bonded system with maximum production, wind farm side, without ground continuity conductor*

From Figure 27, it can be deduced that after removing the ground continuity conductor, the magnitudes of the sheath circulating currents are almost equal. The magnitudes of total sheath circulating currents are approximately 4.9 A in all phases.

Figure 28 presents the simulation results of total sheath circulating currents flowing in the cable between the master turbine and the substation at the substation end of the cable as vector phasors in cross-bonded arrangement.

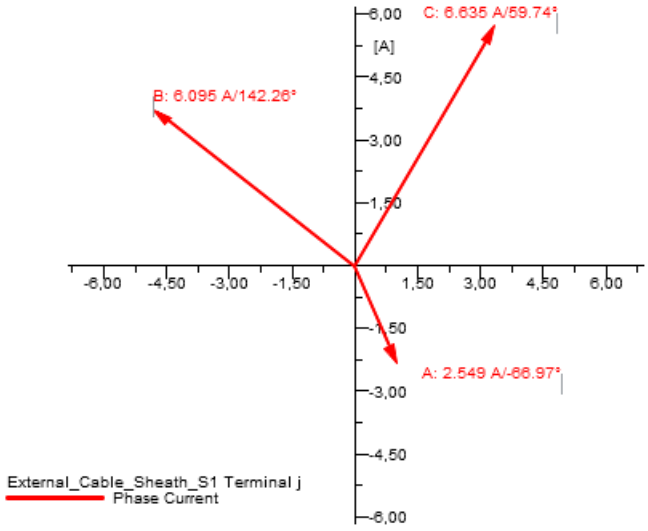

Figure 28. *Sheath current phasors in cross-bonded system with maximum production, substation side*

According to Figure 28, the magnitude of the sheath circulating current in phase A is approximately 2.5 A, in phase B it is approximately 6.1 A and in phase C approximately 6.6 A. From Figure 28, it can be deduced that the magnitudes of the sheath circulating currents in each phase are not equal.

As stated before, the sheaths of the cables are transposed in two locations, the ground continuity conductor is next to phase A sheath at the substation end of the cable. The ground continuity conductor disturbs the symmetrical distribution of the induced currents. Hence, the induced circulating current in each phase increases as the distance from the ground continuity conductor increases.

The conductor currents and the sheath currents are simulated for different output powers of the wind farm to evaluate the magnitude of sheath circulating currents with different conductor currents in cross-bonded arrangement. Based on this evaluation, the effect of implementing cross-bonding to the cabling system can be analysed. The power generation of each turbine is adjusted from 0 MW to 3 MW with 0.5 MW steps.

In the 0 MW situation, the wind turbine generators are disconnected, hence no current is flowing in the conductors. In this situation, no current is induced to the cable sheaths. Hence, the leftover current occurring in the cable sheath depicts the capacitive part of the sheath circulating current.

The results of these simulations are presented in Table 8 and in Figure 29. Abbreviation WF refers to the wind farm and SS refers to the substation. The currents $I_{A,}$ I_B, and I_C denote the simulated currents flowing in conductors of corresponding phases. The currents I_{sa}, I_{sb}, and I_{sc} denotes the simulated currents flowing in sheaths of corresponding phases.

Table 8. *Circulating sheath current simulation results, cross-bonded first case study wind farm*

WTGP injection (MW)	Conductor current WF side (A)			Conductor current SS side (A)			Sheath current WF side (A)			Sheath current SS side (A)		
	I_A	I_B	I_C	I_A	I_B	I_C	I_A	I_B	I_C	I_A	I_B	I_C
0	12.8	12.8	12.8	37.7	37.7	37.7	4.8	5.0	4.9	4.8	4.7	4.9
0.5	84.3	84.4	84.2	78.4	78.5	78.4	5.1	5.0	4.4	4.4	5.1	5.0
1.0	158.9	158.9	158.7	156.5	156.6	156.5	5.3	5.3	4.0	4.0	5.2	5.3
1.5	235.0	235.0	234.8	234.2	234.3	234.1	5.5	5.7	3.7	3.6	5.4	5.6
2.0	311.1	311.2	310.9	311.4	311.5	311.2	5.6	6.1	3.4	3.3	5.6	5.9
2.5	386.9	386.9	386.6	388.0	388.0	387.7	5.9	6.5	3.0	2.9	5.9	6.3
3.0	462.2	462.3	461.9	464.0	464.1	463.7	6.1	6.9	2.8	2.5	6.1	6.6

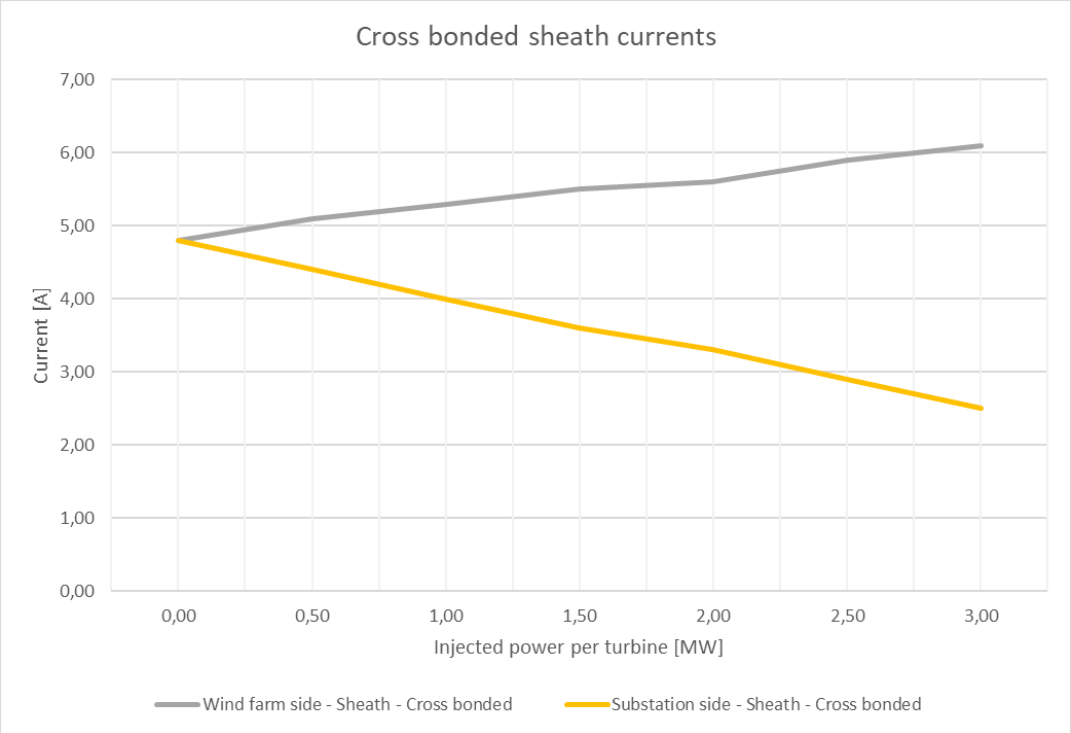

Figure 29 *Circulating sheath current simulation result figures, cross-bonded first case study wind farm*

From the simulation results, it can be concluded that the maximum magnitude of capacitive sheath circulating current has reduced from approximately 13.0 A in solid-bonded arrangement to approximately 4.9 A in cross-bonded arrangement.

The implementation of cross-bonding has significantly reduced the induced sheath circulating currents. Therefore, the total sheath circulating current does not increase significantly with low conductor currents.

The total sheath currents have reduced from a maximum of 54.0 A in solid bonded arrangement to a maximum of 6.9 A in cross-bonded arrangement with maximum production. The implementation of cross-bonding has reduced the sheath circulating currents to acceptable levels, which would not expose the cable to excessive duties.

6.6 Shield current measurements

Shied current measurements have been conducted in the first case study wind farm constructed by ABO Wind. The sheath current measurements were conducted in the cable section between the master wind turbine and the wind farm substation, which suffered joint failures.

Power quality & disturbance recorder PQ-BOX 300 was used to measure the sheath currents at the substation end of the cable. PQ-BOX 150 was used to measure the sheath currents at the wind farm end of the cable. PQ-BOX 100 was used to measure the current flowing in phase 1 conductor. The measurement devices are high-performance portable network- and frequency-analysers combined with a power meter and transient recorders in a single device.

The measurements were conducted during a 10-day period. Figure 30 presents the measurement configuration at the substation end of the cable.

Figure 30. *Sheath current measurement arrangement, substation side*

Figure 31 presents the measurement configuration at the wind farm end of the cable.

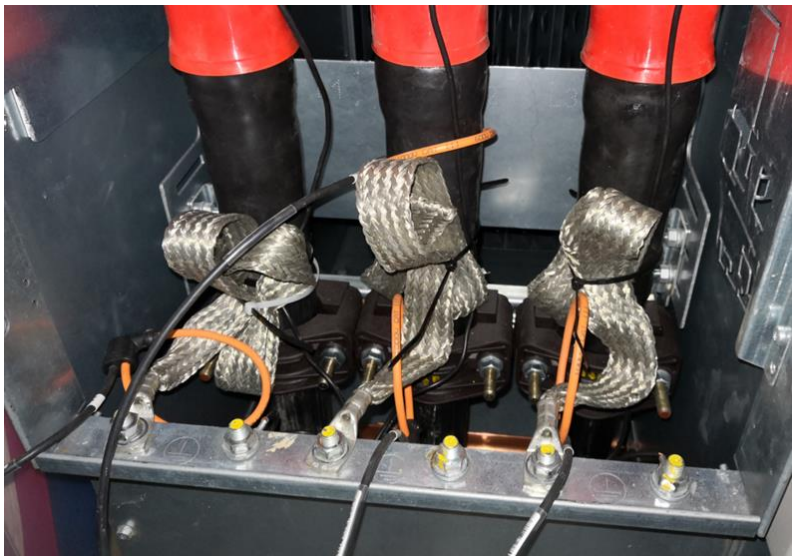

Figure 31. *Sheath current measurement arrangement, wind farm side*

The combined results of the measurement are presented as current as a function of time in Figure 32. The blue graph represents the sheath current measured in phase L1 at the wind farm end of the cable. The grey line represents the sheath current in phase L1 at the substation end of the cable.

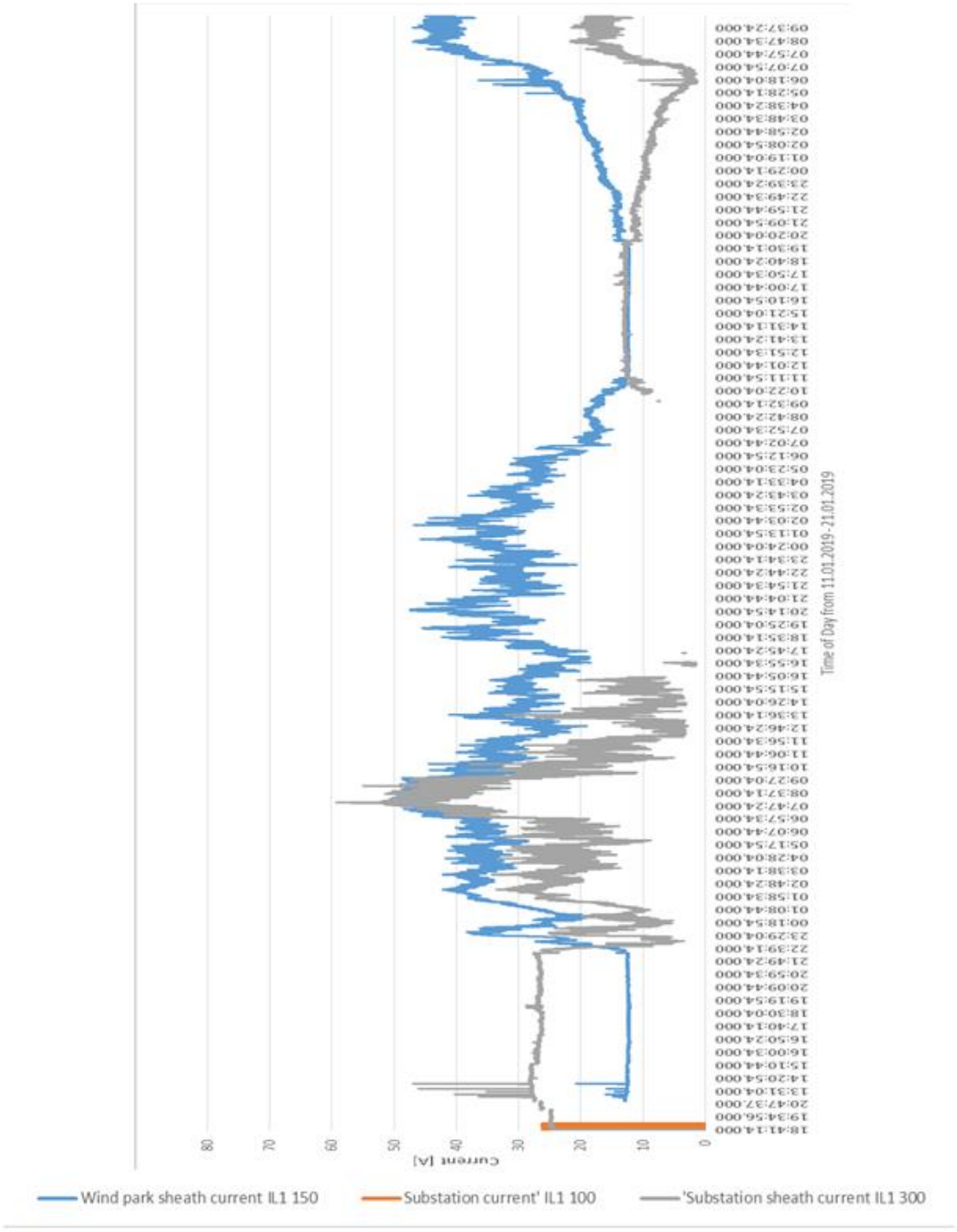

Figure 32. *Combined sheath current measurement results*

From the measurement results, it can be concluded that high sheath currents have been flowing in the cable sheath. The magnitude of sheath current at the substation end of the section has reached almost 60 A and almost 55 A at the wind farm end.

Comparing these maximum values to the current-carrying capabilities of the cable aluminium sheath and the joint braid, it can be deduced that both the sheath and the braid should be able to withstand the sheath circulating currents occurring in the cable.

Nevertheless, an insulation failure occurred during this measurement period on the 21st of January 2019 after the sheath circulating current exceeded 40 A for a two-hour period ending the measurement.

When comparing the measurement results to the simulation results, deviations between the magnitudes of the sheath currents can be observed. There are multiple reasons why the simulated circulating sheath currents deviate from the measured values. For example, the simulation model does not consider the structures of the cable joints. If the simulation model could consider the structural dimensions of the cable joints, the simulated sheath circulating currents could be higher.

Another reason for these deviations could potentially be that in practice, the cable burying formation might have collapsed resulting in increased spacing between the phases. This would lead to greater sheath circulating currents compared to the optimal situation as in the simulation model.

Figure 33 presents the sheath current measurement results as a function of the conductor current of phase L1 at the wind farm side of the cable.

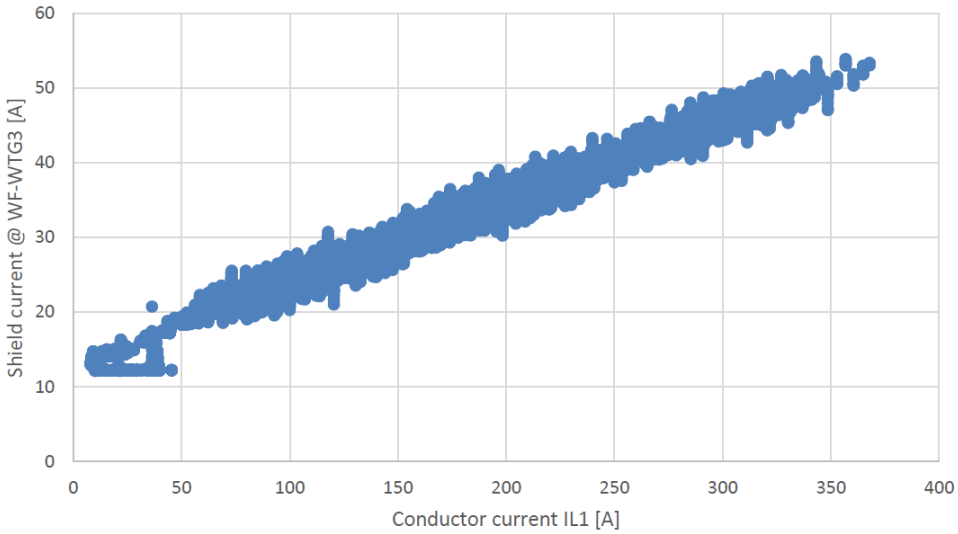

Figure 33. *Sheath current measurement results as a function of conductor current, wind farm side*

From Figure 33, it can be deduced that the magnitude of the total sheath circulating current increases in direct proportion to the conductor current. The wind farm side simulation results presented in Table 7 are in line with the measurement results, considering the relationship between the conductor current and the sheath circulating current. The measurement results indicate that in practice the magnitude of sheath circulating current may exceed 40 A with less than 250 A current flowing in the main conductor.

Figure 34 presents the total sheath circulating current at the substation side of the cable as a function of the conductor current of phase L1.

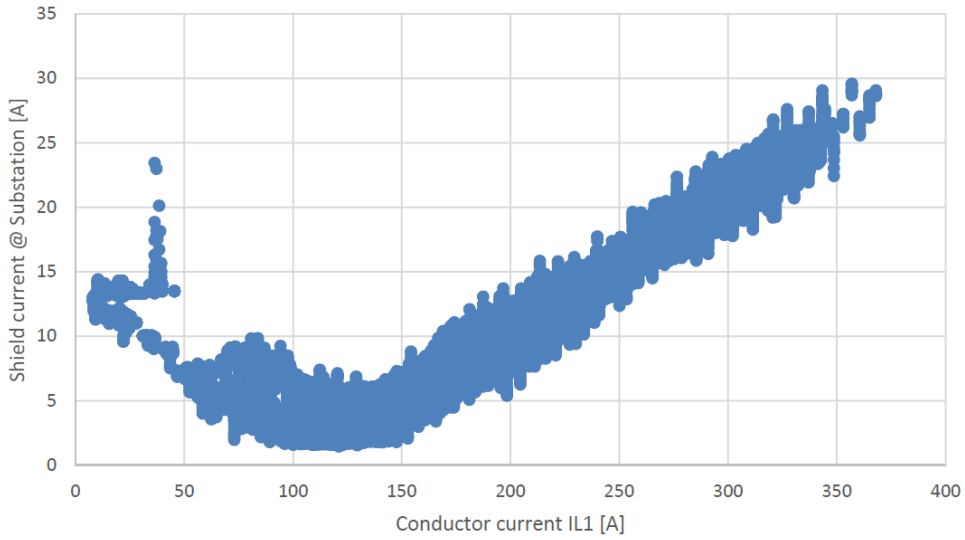

Figure 34. *Sheath current measurement results as a function of conductor current, substation side*

From Figure 34, it can be deduced that the magnitude of the total sheath circulating current begins to decrease as the conductor current increases until the induced part of the sheath circulating current exceeds the capacitive part of the sheath circulating current. The magnitude of the total sheath circulating current begins to increase after this critical point. The substation side simulation results presented in Table 7 are in line with the measurement results, considering the relationship between the conductor current and the sheath circulating current.

According to the measurement results, the maximum magnitude of the total sheath circulating current at the substation side of the cable is 30 A and it does not exceed the proposed limit of 40 A. During the cable lifetime, no faults have occurred at the substation side of the cable. This indicates that a current of 30 A is not high enough to cause excessive heating, which could potentially lead to insulation failures.

According to the measurement results and the laboratory investigations conducted on the faulty joints, a recommendation for limiting the sheath circulating currents to 40 A is proposed in order to avoid joint failures in the medium voltage collector system.

7. CONCLUSIONS

The sheath circulating currents and sheath voltages in power cables exert a significant impact on the design considerations for the wind farm medium voltage collector system. The focus within this thesis has been to review and to develop methods to determine the magnitude of these sheath circulating currents and sheath voltages. Furthermore, other goals were to determine the technical withstand limit of the collector system to these sheath circulating currents and to evaluate methods to decide if mitigation methods are required.

The first case study wind farm has experienced insulation faults in medium voltage transfer cables due to excessive sheath circulating currents combined with impurities inside the cable joints. These failures appeared, even though the medium voltage cable metallic sheaths and medium voltage joint copper braids were designed to withstand the high circulating sheath currents according to their ampacities.

These faults have occurred at the supplying side (wind farm side) of the cable section. Laboratory investigations were performed on these faulty joints. According to the laboratory results, the joints have experienced excessively high sheath circulating currents. The laboratory findings also indicated that impurities have been left inside the finished joint resulting in oxidization within its metallic layers. This has resulted in insufficient connection surface and in heating of the connection between the cable sheath and the joint braid.

These faults have led to high yield losses and high repair costs. Theoretically, one way to mitigate these faults is to limit the sheath circulating currents to acceptable level. A second way of mitigation is to fully avoid the impurities inside the cable joints.

In practice, it is very challenging to fully avoid any impurities to be left inside the cable joints. The joints are often installed in muddy pits in which the impurities are practically unavoidable, even though state of the art installation methods are followed. Therefore, the recommended solution to avoid these joint failures is to mitigate the sheath circulating currents by implementing special bonding methods to the cabling system.

The need for implementing special bonding methods to mitigate the sheath circulating currents must be evaluated in the early phase of planning. In medium voltage cabling systems, the problems occur in the cable joints. Hence, the first criteria for implementing special bonding methods is that the cabling system contains joints.

The second criteria for deciding on bonding methods is by the presence of excessively high sheath circulating currents or voltages. The magnitudes of sheath circulating currents and voltages must be determined at the early phase of planning. The methodology chosen to calculate these currents must be considered carefully, since calculations are

often based on optimal arrangements of the cabling system and the simplified calculations neglect the cable accessories. As the simulation and measurement results in this thesis have indicated, the determined sheath currents can be lower than the actual current flowing in the sheath of the cable.

The need for implementing cross-bonding as mitigation method for high sheath currents, must be based on the magnitude of the total sheath circulating current which is the vector sum of induced and capacitive sheath circulating currents. At the supplying side of the transfer cable, the capacitive and induced sheath circulating currents are in phase and at the receiving side (substation side) they are out of phase.

After the sheath circulating currents are defined, a suitable special bonding method shall be chosen. In this thesis, two special bonding methods were evaluated. For short cabling systems with cable lengths less than 2 km, single-point bonding is a viable option to mitigate the sheath circulating currents. This bonding method fully mitigates the induced sheath circulating currents by breaking the sheath circuit loop. Even though, it introduces a disadvantage as well. It elevates the magnitude of sheath voltage at the unearthed end of the cable. Therefore, the induced sheath voltage must be calculated and compared to the limitations set in the corresponding country.

To provide an example, elevated sheath voltages were calculated for a second case study wind farm. According to the results, the sheath voltage increased from 20.8 V to 30.7 V by implementing single-point bonding to the cabling system. The elevated voltage did not exceed the recommended 65 V limit.

If solid-bonding nor single-point bonding is not a suitable option for the cabling system, cross-bonding should be considered. Cross-bonding mitigates the sheath circulating currents by transposing the cable sheaths in at least two locations along the cable trace. In this thesis, cross-bonding was implemented into the first case study wind farm.

According to simulation results presented in this thesis, implementing cross-bonding to the cabling system reduced the sheath circulating currents from a maximum of 54.0 A to a maximum of 6.9 A granting safe operating conditions for the cable joints. After this implementation, the case study wind farm has not experienced any new failures due to high sheath circulating currents.

Cross-bonding can be used to mitigate high sheath voltage in transfer cables as well. The sheath voltages in the first case study wind farm were calculated using the methods provided in the literature. According to the results, implementing cross-bonding reduced the sheath voltages from 314.3 V to 104.8 V. However, the reduced voltage exceeds the recommended 65 V limit. In countries with limitations to sheath voltages, continuous cross-bonding should be considered to further reduce the sheath voltages.

The cost for implementing cross-bonding to a cabling system is independent of the cable length but the risk of failures in the cable joints due to high sheath circulating currents increase as the cable length increases. Increasing the cable length increases the

capacitive part of the sheath circulating current as well. Hence, the total magnitude of the sheath circulating current increases at the supply side of the cable. Also, the number of joints required in the cable increases as the length of the cable increases. Due to these reasons, the value of investing in a cross-bonding system increases as the length of the cabling system increases.

Due to repeated cable joint failures, sheath current measurements were commissioned to the first case study wind farm. According to these measurement results, a maximum sheath current of almost 60 A has been flowing in the supplying side of the cable section. During the measurement period, the cable experienced an insulation fault inside a cable joint at the supply side. The magnitude of the sheath current progressively exceeded 40 A and stayed on that level for approximately a two-hour period until the fault occurred. On the receiving side of the cable, the magnitude of the sheath current did not exceed 30 A continuously and no faults were experienced.

Based on the sheath circulating current measurements, the joint failures experienced in the first case study wind farm, and on the laboratory findings presented in this thesis, a recommendation for a maximum sheath circulating current of 40 A has been proposed in order to avoid joint failures in wind farm medium voltage collector systems.

REFERENCES

[1] Global Wind Energy Council, “Global Wind Statistics 2017”, 2018

[2] Global Wind Energy Council, ”Global Wind Report 2019”, pp. 13, 2020

[3] European Commission, “A Roadmap for moving to a competitive low carbon economy in 2050”, pp. 1, 2011

[4] Fingrid, “Fingrid debt investor presentation 2016”, pp. 62, 2016

[5] U.S. Department of Energy, “2017 Wind Technologies Market Report”, pp. 25, 2018

[6] ABO Wind, “Track Record”, Available: https://www.abo-wind.com/en/track-record/projects.html (read Dec 2019)

[7] J. Serrano-González, R. Lacal-Arántegui, “Technological evolution of onshore wind turbines – A market-based analysis”, pp. 2174, 2016

[8] International Renewable Energy Agency, ”The Power to Change: Solar and Wind Cost Reduction Potential to 2025”, pp. 16, 2016

[9] U.S. Department of Energy, “2018 Wind Technologies Market Report”, pp. 11, 2019

[10] Finnish Energy Authority, “Preemion tulosten info 2019-03-27”, 2019

[11] W. Thue, “Electrical Power Cable Engineering”, pp. 9, 48, 50-51, 1999

[12] IEEE, “Std. 575-2014 IEEE Guide for Bonding Shields and Sheaths of Single-Conductor Power Cables Rated 5 kV through 500 kV”, pp. 3, 7-21, 24, 36-37, 41, 2014

[13] X.H. Wang, Y.H. Song, C.K. Jung, J.B. Lee, “Tackling sheath problems: Latest research developments in solving operational sheath problems in underground power transmission cables”, in Electric Power Systems Research 77 (2007) 1449-1457, pp. 1450, 2006

[14] L. Kehl, R. Meier, D. Quaggia, “Cross-bonding for MV Cable Systems: Advantages and Impact on Accessories Design”, in 25th International Conference on Electricity Distribution paper n. 37, pp. 1-3, 2019

[15] IEEE, “Std. 575-1988 IEEE Guide for the Application of Sheath-Bonding Methods for Single-Conductor Cables and the Calculation of Induced Voltages and Currents in Cable Sheaths”, pp. 5, 9-10, 27,

[16] M. Santos, M.A. Calafat, “Dynamic simulation of induced voltages in high voltage cable sheaths: Steady state approach”, in Electrical Power and Energy Systems 105 (2019) 1-16, pp. 1-2, 2018

[17] L. Chen, R. Xia, J. Luo, “Technique Research on the Online Detection and Restraint of the Induced Voltage and Circulating Current on the Metal Sheath of 35kV 630mm^2 Single-core XLPE Cable”, in 2010 China International Conference on Electricity Distribution, pp. 1, 4, 2010

[18] H.L. Halvorson, S. Hvidsten, H. Kulbotten, J.K. Lervik, “Experiences with cable faults located at metallic screen connections”, in 24th International Conference & Exhibition on Electricity Distribution 2017 pp. 1, 2017

[19] G. Li, L. Kong, F. Li, D. Xu, “Study on insulation fault of cable joint in an electric field diagnosis technique,” in 2017 International Conference on Computer Systems, Electronics and Control, pp 1-2, 2017

[20] A. Eigner, S. Semino, “50 years of Electrical-Stress Control in Cable Accessories”, DEIS feature article vol. 29, No. 5, in IEEE Electrical Insulation Magazine, pp. 47, 2013

[21] K. Lowczowski, Z. Nadolny, B. Olejnik, “Analysis of Cable Screen Currents for Diagnostics Purposes”, in Energies 2019, 12, 1348 pp. 1-2, 2019

[22] A. Nagaoka *et al.*, “Power System transients; theory and applications.”, CRC Press, pp. 238, 2014

[23] B. D’Andrade, “The Power Grid”, Academic Press, 2017

[24] Sesko standardization in Finland, Standard SFS 6001:2018. Sesko ry, 2018

[25] Energy Networks Association, Standard ENA ER C55-4: Issue 5 2014, Energy Networks Association (UK), 2014

[26] J. Woodworth, “ArresterFacts 032”, pp. 5, 2013

[27] X. Chen *et al.* “Sheath Circulating Current Calculations and Measurements of Underground Power Cables”, in Jicable 2007, 2007

[28] M.N.O. Sadiku, “Elements of electromagnetics”, New York: Oxford University Press, pp. 370, 1995

[29] O.E. Gouda, A. Farag, “Factors Affecting the Sheath Losses in Single-Core Underground Power Cables with Two-Points Bonding Method”, International Journal of Electrical and Computer Engineering vol. 2, No. 1 2012, pp. 9, 2012

[30] Reka Cables, AHXAMK-W 18/30 (36) kV Technical Specification, 2018

[31] A. Ametani, T. Ohno, N. Nagaoka, “Cable System Transients: Theory, Modeling and Simulation”, John Wiley & Sons, Incorporated 2015, pp. 14-15, 2015

[32] O.E. Gouda, A. Farag, “Bonding methods of underground cables”, pp. 36-37, 2015

[33] Sesko standardization in Finland, Standard SFS 6000. Sesko ry, 2017

[34] DIgSILENT GmbH, “Brochure 2020”, pp. 6, 2020

[35] DIgSILENT GmbH, PowerFactory 2020 User manual, pp. 154, 2020

APPENDIX A: REKA CALBES AHXAMK-W DATA SHEET

REKA CABLES

TECHNICAL SPECIFICATION 31.10.2018 LaVa

Page 1/3

AHXAMK-W
18/30 (36) kV

Medium Voltage Aluminium Power Cable

CONSTRUCTION	**CENELEC HD 620 S2:2010 Part 10 Section F applicable parts; SFS 5636:2017 applicable parts**
	This product solution is an individual phase-core of a three-core MV-cable type of AHXAMK-W. This cable type is intended to be installed in trefoil formation with a minimum of 35 mm2 bare earth copper conductor between the three phase-cores. The bare earth copper conductor and each of the metallic screens need to be bonded together at both ends. Earth fault current may be needed taken into consideration in the designing of the electrical network or installation
Phase conductor:	Watertight, circular, stranded and compacted aluminium conductor, IEC 60228 class 2
Conductor screen:	Semiconducting cross-linked polyethylene (XLPE) with nominal thickness of 0,5 mm
Insulation:	Cross-linked polyethylene (XLPE) with nominal thickness of 8,0 mm
Insulation screen:	Semiconducting cross-linked polyethylene (XLPE) with nominal thickness of 0,5 mm
	Conductor screen, insulation and insulation screen are all extruded in the same operation by triple extrusion
Longitudinal watertightness:	Semiconducting water swellable tape applied over insulation screen. Water swellable powder between the conductor wires
Radial watertightness:	PE-laminated aluminium foil bonded to the sheath. Aluminium foil serves also as a metallic shield. Nominal thickness of aluminium foil is 0,3 mm
Oversheath:	Extruded black weather resistant polyethylene sheath, PE-LLD
Rated voltage:	U_0/U (U_m) = 18/30 (36) kV
Temperature limits:	Max. conductor temperature 90 °C Max. short circuit temperature 250 °C (duration not exceeding 5 sec.)
	Min. temperature during handling and installation -20 °C Min. temperature during transport -40 °C
Applications:	Cable is intended for fixed installations outdoors and may also be buried in soil. Cable is both longitudinally and radially watertight and therefore suitable where wet soil and/or water permanently occurs. Suitable for ploughing. Not for submarine or similar applications
Guide to use and selection of cables:	See CENELEC HD 620 S2:2010 Part 10 Section F and SFS 5636:2017

DRYREX

AHXAMK-W

18/30 (36) kV

Technical information	1x300	1x400	1x500	1x630	1x800	1x1000
Product code	**1187090**	**1187091**	**1187093**	**1186015**	**1186013**	**1186011**
Nominal diameter of phase conductor (mm)	20,3	22,5	25,7	29,4	33,3	37,8
Nominal thickness of insulation (mm)	8,0	8,0	8,0	8,0	8,0	8,0
Nominal diameter over insulation without insulation screen (mm)	35,9	38,1	41,3	45,2	49,1	55,0
Nominal thickness of sheath (mm)	2,4	2,5	2,6	2,7	2,8	3,0
Nominal diameter of a sheathed phase conductor (mm)[1]	45	47	51	55	59	65
Weight of cable (kg/km)[1]	2000	2250	2730	3320	4000	4780
Maximum forces during installation when pulling by						
- Pulling-eye (kN)	15,0	20,0	20,0	20,0	20,0	20,0
- Pulling-stocking (kN)	4,5	6,5	7,5	8,5	8,5	8,5
Minimum bending radii						
- During handling and installation, one phase conductor (m)	0,68	0,71	0,77	0,83	0,89	0,98
- In case of only one single smooth bending to final position, one phase conductor (m)	0,47	0,49	0,54	0,58	0,62	0,68
Max. d.c-resistance at 20 °C						
- Phase conductor (Ω/km)	0,100	0,0778	0,0605	0,0469	0,0367	0,0291
AC-resistance of phase conductor, screen circuit closed[1]						
- Conductor temperature 40 °C (Ω/km)	0,109	0,086	0,068	0,054	0,043	0,036
- Conductor temperature 65 °C (Ω/km)	0,119	0,093	0,073	0,058	0,047	0,039
- Conductor temperature 90 °C (Ω/km)	0,129	0,101	0,079	0,063	0,050	0,041
Inductance per phase in trefoil (mH/km)[1]	0,34	0,33	0,32	0,31	0,30	0,29
Capacitance (µF/km)[1]	0,24	0,26	0,29	0,32	0,36	0,41
Charging current (A/km)[2]	1,3	1,4	1,6	1,8	1,9	2,2
Earth fault current (A/km)[2]	3,6	4,2	4,7	5,3	5,8	6,7
Current ratings in trefoil (according to CENELEC HD 620 S2 2010 Part 10F and SFS 5636) when screen circuit is closed						
- Cables in air 25 °C, conductor temperature 90 °C (A)	565	680	775	880	1010	1130
- Cables in ground (15 °C and 1,0 Km/W), installation depth 0,7 m, conductor temperature 40 °C (A)	320	375	420	470	525	580
- Cables in ground (15 °C and 1,0 Km/W), installation depth 0,7 m, conductor temperature 65 °C (A)	435	510	570	635	695	760

DRYREX

	1x300	1x400	1x500	1x630	1x800	1x1000
Product code	**1187090**	**1187091**	**1187093**	**1186015**	**1186013**	**1186011**
Maximum 1 second thermal short-circuit current						
- Phase conductor (temp. at the beginning 90 °C, final temperature 250 °C) (kA)	28,3	37,8	47,2	59,5	75,6	94,5
- Metallic screen (temp. at the beginning 35 °C, final temperature 250 °C) (kA)	6,2	6,4	7,1	7,6	8,3	9,3
- Metallic screen (temp. at the beginning 60 °C, final temperature 250 °C) (kA)	5,7	5,9	6,6	7,0	7,7	8,6
- Metallic screen (temp. at the beginning 85 °C, final temperature 250 °C) (kA)	5,2	5,4	6,0	6,4	7,0	7,8

1) Calculated value, for guidance only
2) Calculated value for guidance, with operational voltage U = 30 kV

DRYREX